

# **Hydrate Formation in Multiphase Flow in Pipe**

By

**Seng Sook Harn**

**12842**

Interim Report submitted in partial fulfillment of

The requirements for the

Bachelor of Engineering (Hons)

(Mechanical Engineering)

AUGUST 2013

Universiti Teknologi PETRONAS  
Bandar Seri Iskandar  
31750 Tronoh  
Perak Darul Ridzuan

# Hydrate Formation in Multiphase Flow in Pipe

By

Seng Sook Harn

A project dissertation submitted to the  
Mechanical Engineering Programme  
Universiti Teknologi PETRONAS  
in partial fulfillment of the requirement for the  
BACHELOR OF ENGINEERING (Hons)  
(MECHANICAL ENGINEERING)

Approved by,

---

(Dr. Aklilu Tesfamichael)

Approved by,

---

(Dr. William Pao)

UNIVERSITI TEKNOLOGI PETRONAS

TRONOH, PERAK

August 2013

## **CERTIFICATION OF ORIGINALITY**

This is to certify that I am responsible for the work submitted in this project, that the original work is my own except as specified in the references and acknowledgements, and that the original work contained herein have not been undertaken or done by unspecified sources or persons.

---

SENG SOOK HARN

## **ABSTRACT**

Hydrate blockage in pipelines is a serious problem to the oil and gas industries. Hydrate formation occur in pipelines which are under high pressure and fairly low temperature, most frequently encountered in deep sea oil and gas production. Plugged-up pipelines cast impacts on the fluid multiphase flow in pipes such as pressure drop and decreased flow rate. Specifically, this research's objectives are firstly i) to develop multiphase model of the hydrate formation and deposition inside a multiphase flow pipe and ii) to investigate the effect of different inlet velocity, hydrates particles diameter, interfacial area density and flow viscosity on the hydrate formation and plugging behavior in pipelines. This research had performed modeling on the multiphase flow and hydrate growth using ANSYS CFX. The two objectives were met at the end of the project as a multiphase model which is able to represent the hydrate formation in multiphase flow pipe was developed. Also, the relationship between flow inlet velocity, hydrates particle diameter, interfacial area density and flow viscosity variation and the hydrate formation and plugging behavior in pipelines had been determined. Knowledge obtained from the research serves to further improve the oil and gas industry nowadays by maximizing its profit margin through implementation of hydrate plug-free pipelines.

# TABLE OF CONTENTS

CERTIFICATE OF ORIGINALITY .....	i
ABSTRACT.....	ii
CHAPTER 1: INTRODUCTION .....	1
1.1 Project Background .....	1
1.2 Problem Statement .....	2
1.3 Objective of Study.....	2
1.4 Scope of Study .....	2
CHAPTER 2: LITERATURE REVIEWS .....	3
2.1 Gas Hydrates Kinetic .....	3
2.2 Hydrates Plugging Scenario .....	5
2.3 Hydrate Shell Model .....	6
2.4 Hydrate Formation Condition .....	9
2.5 Factors Affecting Hydrate Formation and Pipe Plugging.....	10
2.6 Gas Hydrates Equilibrium Conditon.....	12
2.7 Hydrates Particle Aggregation .....	13
CHAPTER 3: METHODOLOGY .....	14
3.1 Research Methodology.....	14
3.2 Modeling Methodology.....	15
3.2.1 Geometry Setup	
3.2.2 Mesh Generation	
3.2.3 Fluid Setup	
3.2.4 Multiphase Model	
3.2.5 Boundary Conditions	
3.2.6 Turbulence Model	
3.2.7 Particle Model	
3.3 Multivariate Regression Analysis .....	20
3.4 Parametric Analysis .....	21
3.5 Project Flow Chart .....	22
3.6 Gantt chart.....	24
CHAPTER 4: RESULTS AND DISCUSSION.....	25
4.1 Model Validation Results and Discussion .....	25
4.2 Regression Analysis .....	28

4.3 Hydrate Formation and Deposition Simulation .....	30
4.4 Effect of Hydrate Particle Size on Hydrate Formation .....	33
4.5 Effect of Interfacial Area Density on Hydrate Formation .....	35
4.6 Effect of Inlet Velocity on Hydrate Formation .....	38
CHAPTER 5: CONCLUSION AND RECOMMENDATION .....	41
REFERENCES.....	43

## LIST OF FIGURES

Figure 2.1 Main stages of hydrate formation .....	3
Figure 2.2 Nucleation on a distinct solid surface (I) and on an interphase between hydrocarbon and aqueous phases (II). .....	4
Figure 2.3 Gas hydrate formation in a liquid-dominated system.....	5
Figure 2.4 Gas hydrate formation in a gas-dominated system.....	6
Figure 2.5 Gas hydrate formation in a gas-dominated system.....	7
Figure 2.6 Hydrate-formation curve for various gas gravities.....	9
Figure 2.7 Required subcooling for methane (gas A0 and a natural gas (gas C).....	10
Figure 2.8 Comparison of the gas inclusion rates for two different natural gases.....	11
Figure 2.9 Hydrate equilibrium curves for methane and a gas mixture (obtained using computer program from CSMhyd 1998). .....	12
Figure 2.10 Spatially averaged hydrate particle diameter as a function of mean velocity. .. .....	14
Figure 3.1 The three-dimensional CAD-model used in the study. ....	16
7Figure 3.2 Grid generation on the surface of the pipe.....	17
Figure 4.1 Graph of hydrate precipitates/bed thickness against mean flow velocity. Comparison of ANSYS CFX, experimental data and study by Fatnes.. .....	27
Figure 4.2 Sensitivity of different parameters to hydrate thickness formed in multiphase flow pipe. Results obtained from experimental design and second order regression. ....	28
Figure 4.3 Significance of factors on hydrates thickness formed in the pipe. ....	30
Figure 4.4 Contour of the hydrate volume fraction at midline cross-section of the pipe. Mean inlet velocity of 0.1 m/s, particle size of 0.0033 m. ....	31
Figure 4.5 Figure 4.5 Contour of the water (continuous phase) velocity at midline cross-section of the pipe. Mean inlet velocity of 0.3 m/s, particle size of 0.0035 m, interfacial area density of 0.075 and viscosity of 0.0061. ....	31
Figure 4.6 Effect of hydrates particle size on hydrates thickness for condition i.) .....	33

Figure 4.7 <i>Effect of hydrates particle size on hydrates thickness for condition</i> <i>ii.)</i> .....	34
Figure 4.8 <i>Effect of hydrates particle size on hydrates thickness for condition</i> <i>iii.)</i> .....	34
Figure 4.9 Effect of interfacial area density on hydrates thickness for 0.00465 kg/ms viscosity, 0.003m particle diameter, 0.2m/s to 0.4m/s inlet velocity. ....	36
Figure 4.10 Effect of interfacial area density on hydrates thickness for 0.00465 kg/ms viscosity, 0.002m particle diameter, 0.2m/s to 0.4m/s inlet velocity ....	37
Figure 4.11 Effect of interfacial area density on hydrates thickness for 0.00755 kg/ms viscosity, 0.002m particle diameter, 0.2m/s to 0.4m/s inlet velocity ....	37
Figure 4.12 Effect of inlet velocity on hydrates thickness for 0.00755 kg/ms viscosity, 0.002m to 0.0035m particle diameter, 0.088 min. area density .....	39
Figure 4.13 Effect of inlet velocity on hydrates thickness for 0.00610 kg/ms viscosity, 0.0015m to 0.0035m particle diameter, 0.075 min. area density .....	39
Figure 4.14 Effect of inlet velocity on hydrates thickness for 0.00465 kg/ms viscosity, 0.002m to 0.0035m particle diameter, 0.063 min. area density .....	40



# CHAPTER 1

## INTRODUCTION

### 1.1 Project Background

Hydrate is formed when a water molecule is added to a base molecule, producing another molecule with different properties. The water molecules could either become a part of the base molecule structure or being attached to the center of the base molecule.

In oil and gas industries, hydrates are found in the form of natural gas hydrates. Gas hydrates (Clathrates) are crystalline compounds consisting of an ice-like water lattice with a “guest” molecule trapped. The water molecules form hydrogen bonds and with pressure increasing, these water molecules are driven together and produce a polyhedron with a lattice hole that traps gasses such as methane, ethane, propane, and other higher molecular weight hydrocarbons (Donohoue, 2000).

According to an Offshore magazine article, the writer portrayed hydrates as crystals that form in high-pressure and low-temperature flows where water and natural gas are present. As the natural gas becomes encased in a lattice of ice formed from the water, these hydrates will cause blockages in tubing, flow lines, and pipelines (Cahill, 2011).

Multiphase flow occurs in almost all producing oil and gas wells and surface pipes that transport produced fluids. Multiphase flow is defined as simultaneous flow of matter of different states or phases, for example gas, liquid or solid. Besides, multiphase flow is also interpreted as simultaneous flow containing matter at the same phase but with different chemical properties. Due to the variation in the matter states and chemical properties, temperature and pressure tend to vary throughout the flow in pipe. When the situation reaches the favorable temperature and pressure for hydrate formation, ice or wax mixture would be produced which creates a choking barrier around the circumference of the pipe.

## **1.2 Problem Statement**

Hydrate is a form of crystalline compound consisting ice-like water lattice or wax mixture that under favorable temperature and pressure forms a choking barrier around the circumference of the pipe, obstructing the flow. This situation is mostly encountered in deep sea oil/gas pipe where the subsea temperature is very cold. When there are hydrates formation in a pipeline, changes in fluid rates and compositions at the separator would be observed. Pressure drop also increases while flow rate decreases when the pipe diameter is decreased by hydrate formation at the wall in a pipeline. It also shut the gas flow rate partially or completely in well bore, well top pipes, system of field pipelines and installations. These impacts would hinder the oil / gas transportation and production process and lower the plant's productivity and revenue. Therefore, there is a need to investigate the growth of the hydrate layer around the inner circumference of the multiphase flow pipe.

## **1.3 Objective of Study**

The objectives of this study are stated as below:

1. To develop multiphase model of the hydrate formation and deposition inside a multiphase flow pipe
2. To investigate the effect of different inlet velocity, hydrates viscosity and hydrates particles diameter on the flow and plugging behavior in pipelines

## **1.4 Scope of Study**

This study is restricted to:

1. Restricted to gas-slurry two phase flow and its behavior in pipes
2. Restricted to liquid-dominated system
3. Multiphase flow is based on assumption that the fluid is a gas-slurry stratified flow
4. Restricted to isothermal heat transfer model.

## CHAPTER 2

### LITERATURE REVIEW

#### 2.1 Gas Hydrates Kinetic

Hydrate formation are separated into two main stages: hydrate nucleation and hydrate growth. Hydrate formation is initiated by nucleation where a solid pre-hydrate crystal/nucleus would be created. At this stage, the nucleus is unstable due to the energy demand for the nucleus to build onto its own surface. (Balakin, 2010)

Figure 2.1 summarizes the main stages of hydrate formation which starts from nucleation until hydrates growth and their key properties.

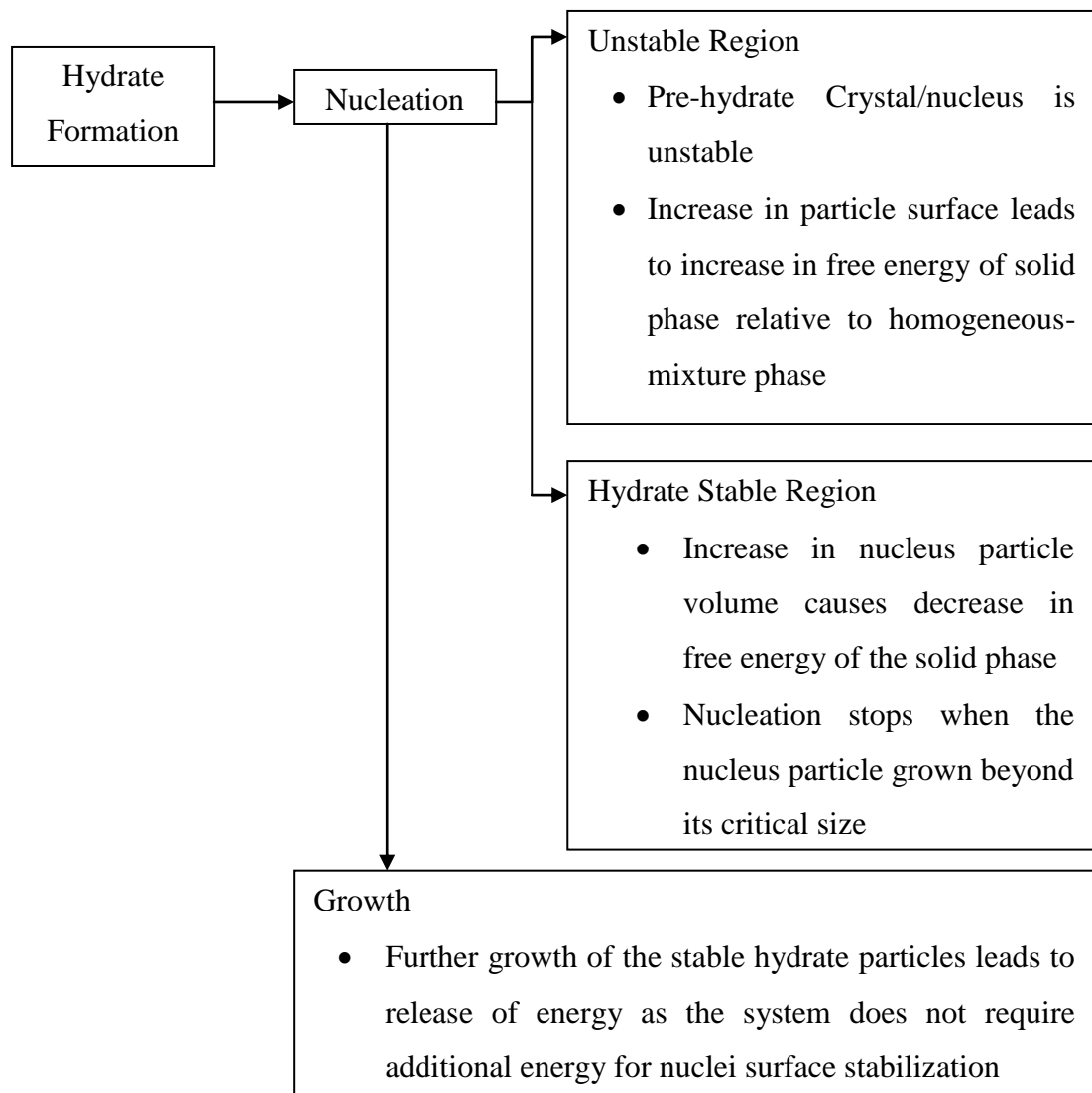


*Figure 2.1 Main stages of hydrate formation.*

Assuming the hydrate particles to be spherical, Gibbs free energy of the solid phase relative to the homogeneous solution is given by Equation 2.1:

$$\Delta G_{hom} = \frac{4}{3} r^3 \pi G_v - 4\pi r^2 \sigma \quad (2.1)$$

Where,  $\Delta G_{hom}$  is the change of Gibbs free energy of the system upon dissolution of the particles if no impurities are present. From Equation 2.1, the critical size,  $r_{cr}$  of the pre-hydrate particle at which the energy of the system is at an extremum can be obtained as:

$$r_{cr} = \frac{2\sigma}{G_v} \quad (2.2)$$

The nucleation process above is an idealized case of homogeneous nucleation which occurs in highly supersaturated systems. However, there are conditions where there are impurities in the system such as solid contaminant, liquid droplet or gas bubble. The solution is then known as heterogeneous solution and these impurities may form the center of heterogeneous nucleation. According to Boris V. Balakin, the energy gain for the hydrate nucleation on the impurities' surface is lower compared to that in homogeneous nucleation. The free energy equation for heterogeneous nucleation is shown in Equation 2.3:

$$\Delta G_{het} = f(a, b, c) \Delta G_{hom} \quad (2.3)$$

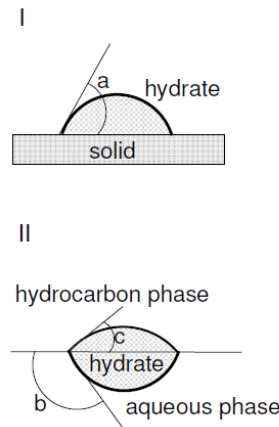


**Figure 2.2** Nucleation on a distinct solid surface (I) and on an interphase between hydrocarbon and aqueous phases (II). (Boris V. Balakin, 2010)

---

$G_v$  is the energy release due the formation of solid per unit volume;  $r$  is the radius of hydrate nuclei;  $\sigma$  is the energy gain for the formation of new surface per unit surface;  $f(a, b, c)$  is a correction factor, which depends on the contact angles  $a, b, c$  between the tangential line to the nuclei surface and the interphase (Figure 2.2).

## 2.2 Hydrates Plugging Scenario

Hydrates formation occur differently in different systems. In a liquid-dominated system, hydrates form on the interface between the oil and aqueous phases, usually occurs on the water droplets dispersed in the oil phase. During the inter-phase, solid shell would be form around the water droplets and further converted to hydrates particles. However, the hydrates formation is rather slow due to the low diffusion rate of gas molecules through the shell. (Balakin, 2010)

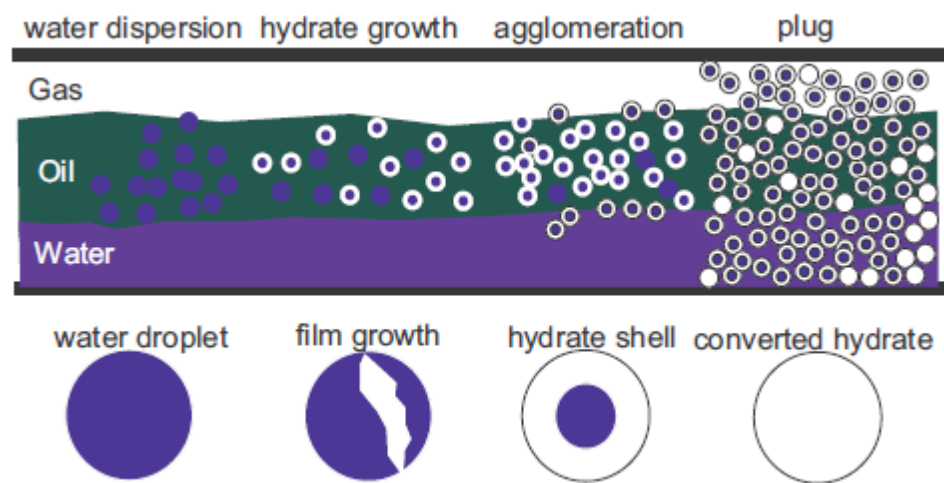


**Figure 2.3** Gas hydrate formation in a liquid-dominated system. (Balakin,2010)

Presence of hydrates particles in the system increases the viscosity of a solid-liquid slurry flow. Consequently, pressure loss due to frictions in the system is increased and causes the flowing solid particles to aggregate and further increase the flow viscosity. The aggregates form large assemblies as time pass by until the system reaches a state where the system agitators in the flow fail to overcome the frictional resistance. Thus, the aggregates are joined together and plug the pipeline. There are also cases where the hydrate-covered water droplets' shells are broken due to the inter-particle or particle-wall collisions and turbulent pulsations in the carrier flow. This would enhance hydrate growth in the system.

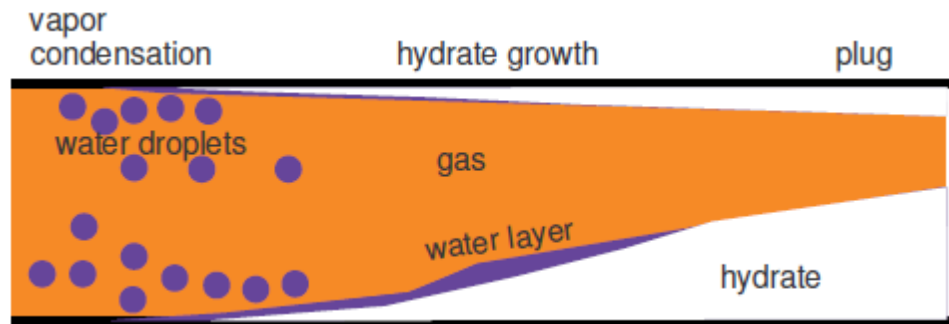


**Figure 2.4** Gas hydrate formation in a gas-dominated system. (Balakin,2010)

On the other hand, the hydrates formation process occurs in a different way for a gas-dominated system. In natural gas industry pipelines, water exists as vapor. When the natural gas is being transferred in subsea, the ambient temperature is often lower than the equilibrium temperature for gas-water vapor flow. Due to this, condensation of water occurs on the walls of the pipelines, thus producing a gas-liquid flow. In contrast to liquid-dominated system, the hydrates are formed on the pipe walls instead of having the hydrates particles to form in bulk. As shown in Figure 2.4, the hydrates particles formed from condensation form a monolith hydrate layer from the pipe walls. Further condensation on the hydrate layer makes it thicker and plugging the pipeline.

### 2.3 Hydrates Shell Model

Considering a multiphase flow model which assumes that the flow is in a stratified regime, regardless of the hydrates form or not, it is assumed that the hydrate particles are formed at interface between oil and water droplet and then dispersed in the oil phase. The hydrate formation is described using a hydrate shell model developed through numerical simulation by Gong, Shi and Zhao. (Gong *et al.*, 2010)

In developing the hydrate shell model, it is assumed that the hydrate shell is at the same temperature as the hydrate-water interface. Secondly, the heat released from hydrate formation is transferred only via the water phase. The phase equilibrium was assumed to be established instantly. Besides that, it is also assumed that the gas content is higher than water. Therefore, the system still exists as a gas-liquid flow even if the water is totally converted to hydrates.

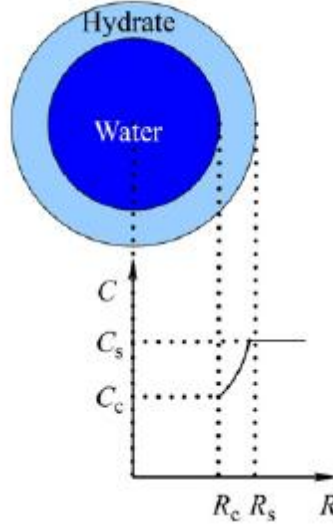


**Figure 2.5** Gas hydrate formation in a gas-dominated system. (Gong *et al.*, 2010)

Gong *et al.* (2010) focused on four main components in the hydrate shell growth model which are i) gas diffusion through the hydrate shell, ii) gas consumed in hydrate kinetic model, iii) water consumed in core of hydrate shell, and iv) gas mass balance at the surface of hydrate shell.

### I. Gas Diffusion through the hydrate shell

Based on Fick's second law, the quasi-steady diffusion equation is formulated as below:

$$\frac{d}{dr} \left( r^2 \frac{dC}{dr} \right) = 0, R_c \leq r \leq R_s \quad (2.4)$$

With the boundary equations of,

$$C(R_c) = C_c$$

$$C(R_s) = C_s$$

Analytical solution to equation 2.4 with the boundary equations above gives the gas molecules diffusion rate at the interface as

$$M_1 = \frac{dn}{dt} = 4\pi R_s^2 D_{eff} \frac{dC}{dr} \Big|_{r=R_s} = -4\pi D_{eff} \frac{C_c - C_s}{\frac{1}{R_c} - \frac{1}{R_s}} \quad (2.5)$$

---

$C$  is the concentration of gas;  $R_c$  is the radius of water droplet;  $R_s$  is the radius of hydrate shell;  $C_c$  is the gas concentration at  $R_c$ ;  $C_s$  is the gas concentration at  $R_s$ ;  $M_1$  is the gas consumption rate calculated by hydrate shell model;  $D_{eff}$  is the diffusion coefficient.

## II. Gas consumed in hydrate kinetic model

Number of moles of gas consumed per particle per second is given by:

$$\frac{dn}{dt} = KA_p(f - f_{eq}) \quad (2.6)$$

Assuming the number of moles of water remains practically constant, the concentration of gas expressed in terms of its fugacity,

$$f = H \frac{C_i}{C_i + C_{w0}} \approx H \frac{C_i}{C_{w0}} \quad (2.7)$$

Where H is the Henry's law constant, which depends on the solute, solvent and temperature.

At the interface, equation 2.7 is expressed as

$$M_2 = \frac{d}{dt} = KA_p H \frac{C_c - C_{eq}}{C_{w0}} = 4\pi R_c^2 KH \frac{C_c - C_{eq}}{C_{w0}} \quad (2.8)$$

## III. Water consumed in core of hydrate shell

Water consumption rate is in proportion to the radius of the water droplet and is expressed as:

$$r_w = \frac{d}{dt} \left( \frac{4}{3} \pi R_c^3 \frac{\rho_w}{M_w} \right) = 4\pi R_c^2 \frac{\rho_w}{M_w} \frac{dR_c}{dt} \quad (2.9)$$

## IV. Gas mass balance at the surface of hydrate shell

In the quasi-steady condition during the unit intervals, it is assumed that the gas molecules diffusing through the hydrate shell equal to the gas molecules consumed around the water droplets' surface. Besides, it is in proportion to the water molecules consumed.

$$M_1 = M_2 = \frac{(-r_w)}{\lambda} \quad (2.10)$$

Combining equations 2.5, 2.8, 2.9 and 2.10 leads to the expression below:

$$\frac{dR_c}{dt} = - \frac{\lambda M_w D_{eff} (C_s - C_{eq})}{\rho_w \left[ \frac{D_{eff} C_{w0}}{KH} + \left( \frac{1}{R_c} - \frac{1}{R_s} \right) R_c^2 \right]} \quad (2.11)$$

---

K is the combined rate parameter; H is the Henry's law constant;  $A_p$  is the hydrate shell surface area;  $C_i$  is the gas concentration at the hydrate-water interface;  $C_{w0}$  is the concentration of water;  $f$  is the fugacity of gas at the system pressure and temperature;  $f_{eq}$  is the fugacity of gas at equilibrium;  $M_2$  is the gas consumption rate calculated by hydrate kinetic model;  $r_w$  is the water consumption rate;  $\lambda$  is the hydrate structure constant;  $M_w$  is the molar mass of water;  $\rho_w$  is the water density;  $C_{eq}$  is the gas concentration at equilibrium.



## 2.4 Hydrate Formation Conditions

Sloan (2000) stated that for hydrates to form, free water and natural gas components must be present. Free water for hydrates formation can be from the reservoir or condensation from cooling the hydrocarbon fluid. Hydrates formation requires low temperature condition. However, even though hydrates are made up of 85 % mol of water, the system temperature does not need to be below 32 °F or water freezing point for hydrates to be formed. In offshore operations, below approximately 3,000 ft of water depth would have an uniform ocean-bottom temperature at 38 °F to 40 °F. At 38 °F, common natural gases form hydrates at pressure as low as 100psig. At a high pressure of 1500 psig, hydrates formation could occur at a temperature of 66 °F. (Sloan Jr, 2000)

Knowing the gas component in a pipeline allows the identification of the hydrates formation pressure given the temperature, and vice versa, with the aid of gas gravity chart for the specific gas involved. The gas gravity chart should be able to provide the mole fraction, molecular weight, and fraction molecular weight of each component. The following gas-gravity equation is used:

$$\gamma_g = \frac{M_g}{M_a} \quad (2.12)$$

With the gas gravity from Equation 2.12 and temperature known, the pressure for hydrates formation can be obtained from the graph in Figure 2.6 below.

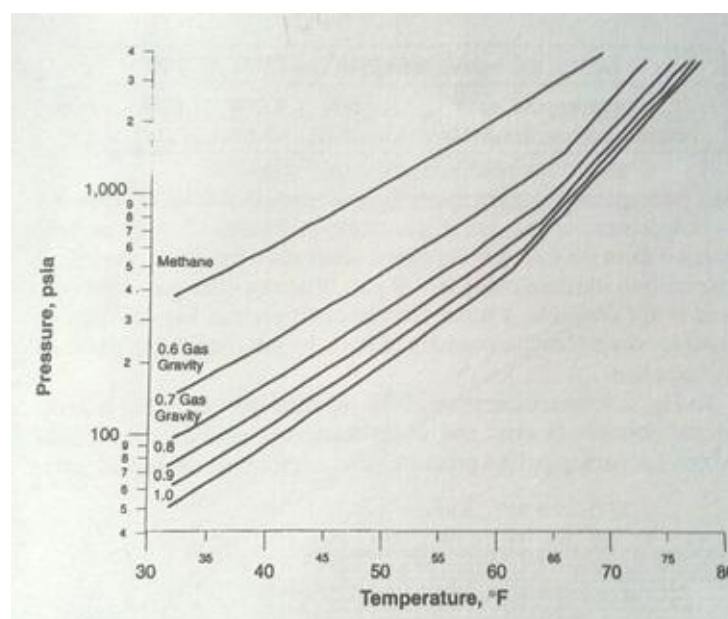


**Figure 2.6** Hydrate-formation curve for various gas gravities. (Sloan Jr, 2000)

## 2.5 Factors Affecting Hydrate Formation and Pipe Plugging

As an effort to study on hydrate formation kinetics, an experiment was conducted to investigate the duration of the induction period and the hydrate growth rate as a function of flow velocity and gas composition. Induction time is defined as the duration of the nucleation phase and it is influenced by several parameters including the level of subcooling (Englezos, 1987a) and the guest to cavity size ratio (as suggested by Sloan and Fleyfel, 1991). In the experiment, there were four types of natural gas being studied which are pure methane (gas A), methane/ethane mixture (gas B), natural gases (gas C and D). Gas C contains more ethane and propane as compared to gas D which has more nitrogen. Lipmann *et.al.* (1995) found that methane and natural gas C show different behavior in which the induction time is longer than for the natural gas C than that of methane for all flow velocities, as shown in figure 2.7. This is due to the different hydrate structures formed from the two gases thus indicating gas composition greatly affects the hydrate formation and pipe plugging.

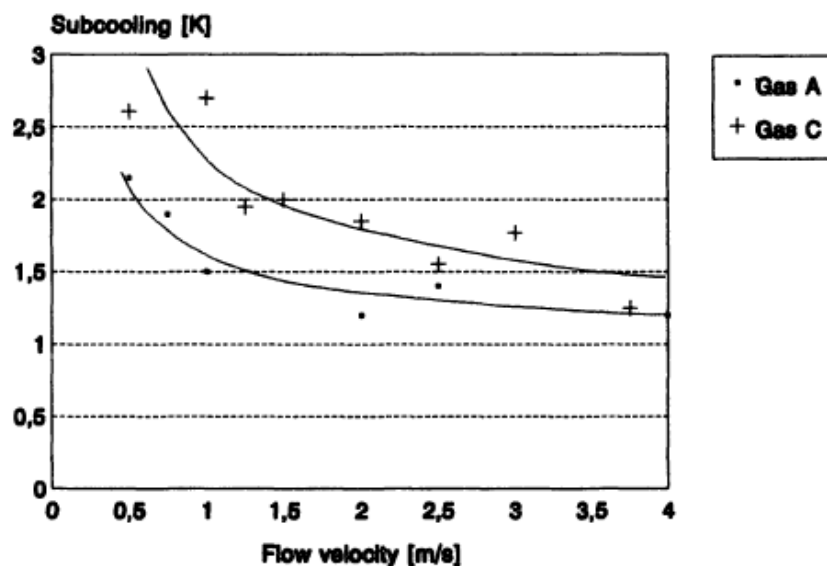


*Figure 2.7* Required subcooling for methane (gas A) and a natural gas (gas C).  
(Lipmann *et al.*, 1995)

Lipmann *et.al.* (1995) also investigated the hydrate growth rate by determining the gas consumed to be incorporated in to the hydrate structure and how it is affected by the flow velocity. From figure 2.8, it can be observed that a significant increase of

the hydrate growth with increasing flow velocity when the flow velocity is up to 4.5m/s. This is due to an increased mass transfer at the gas-water interface and also an enhanced heat transfer via convection. Figure 2.8 also showed the dependence of hydrate growth rate on the gas composition. For example, the gas C has a higher hydrate growth rate due to the ethane and propane contents which are able to stabilize the hydrates structures better than gas D. Again, it is proven that gas composition and flow velocity cast a great influence on hydrate formation.

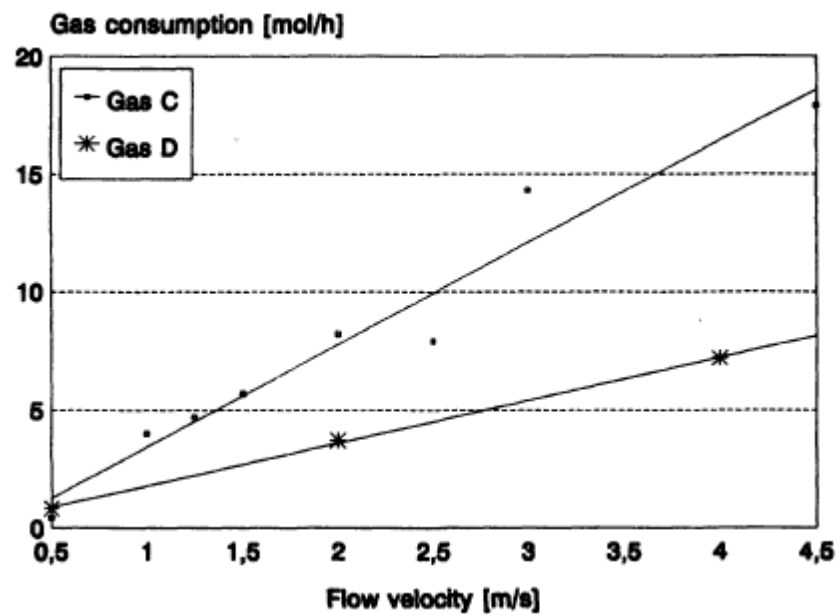


*Figure 2.8 Comparison of the gas inclusion rates for two different natural gases. (Lipmann et al., 1995)*

Aspenes *et al.* (2009) stated that hydrate's tendency to stick to the surface depends on the pipe surface's wettability. Wettability is measured by droplets' tendency to wet the surface. This model indicates that surface changes, for example surface treatment or corrosion, would also influence the hydrate blockage tendency. Increased surface roughness is believed to be a contributing factor in speeding up hydrate formation.

Ova Bratland (2010) also stated that hydrate formation is influenced by fluid flow where the interaction between phases in the different flow regimes varies. The rate of hydrate formation and dissociation is governed by the mixing rate, the surface area between the hydrocarbon-rich phase and water, and lastly the temperature. In the

book, the author had included hydrate curves for various pure components which illustrate the hydrate growth of various components such as propane, hydrogen sulfide and methane under a range of pressure and temperature variation. (Bratland, 2010)

## 2.6 Gas Hydrates Equilibrium Condition

The pressure and temperature conditions for hydrate formation depend on the water and the gas composition. Computer programs are used for prediction of the hydrate equilibrium line, which is the line in the pressure-temperature diagram that defines the hydrate forming area. By using statistical thermodynamics, the hydrate formation equilibrium pressure for a gas and a water phase can be computed given the temperature, or vice versa. (Andersson, 1999)

A computer program which was developed at the Colorado School of Mines (CSMhyd 1998) was used to obtain the hydrate equilibrium lines for two gases which are methane (Structure I) and a gas mixture (Structure II). The equilibrium lines are portrayed in Figure 2.9.

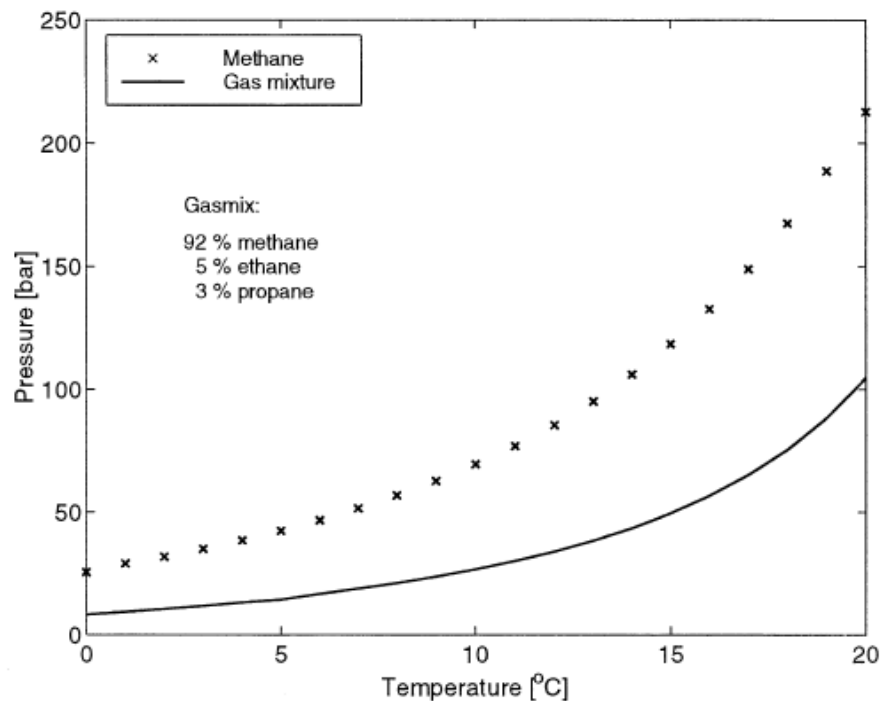


*Figure 2.9 Hydrate equilibrium curves for methane and a gas mixture (obtained using computer program from CSMhyd 1998).*

Based on Figure 2.9, the equilibrium lines separate hydrate stable region from hydrate dissociates region. It is observed that at high pressures or above the equilibrium lines, the hydrates are stable. On the other hand, hydrates will dissociate at conditions under the lines. The equilibrium pressure for the gas mixture of 92% methane, 5% ethane, and 3% propane at 0 °C is 8.2 bar whereas for methane, the equilibrium pressure is at 25.5 bar. However, when the temperature is below 0 °C, equilibrium thermodynamics alone can no longer describe the natural gas hydrates system. Hydrates are meta-stable at atmospheric pressure in cases where the temperature is kept below 0 °C.

## 2.7 Hydrates Particles Aggregation

Hydrates particle size is significantly influenced by aggregation and breakage, related to shear in the flow. It is not only the result of hydrate particle evolution in the pipeline but also includes the effect from the upstream feed pump. Particle size distribution is depended on the flow parameters and their cohesive properties.

$$d_h = \left( \frac{F_a(d_1)^{2-fr}}{\mu_w \gamma} \right)^{\frac{1}{4-fr}} \quad (2.13)$$

Where,  $d_h$  is the hydrate aggregate diameter,  $\gamma$  the shear rate and some parameters determined by the series of population balance simulations:  $d_1 = 7 \mu\text{m}$  which is the diameter of the hydrate primary particle,  $F_a = 1.75 \text{ nN}$  which is the floc adhesion force and  $fr = 1.83$  which is the aggregate fractal dimension. (Mühle, 1993)

The particle size as a function of the mean flow velocities is given in Figure 2.10 below.

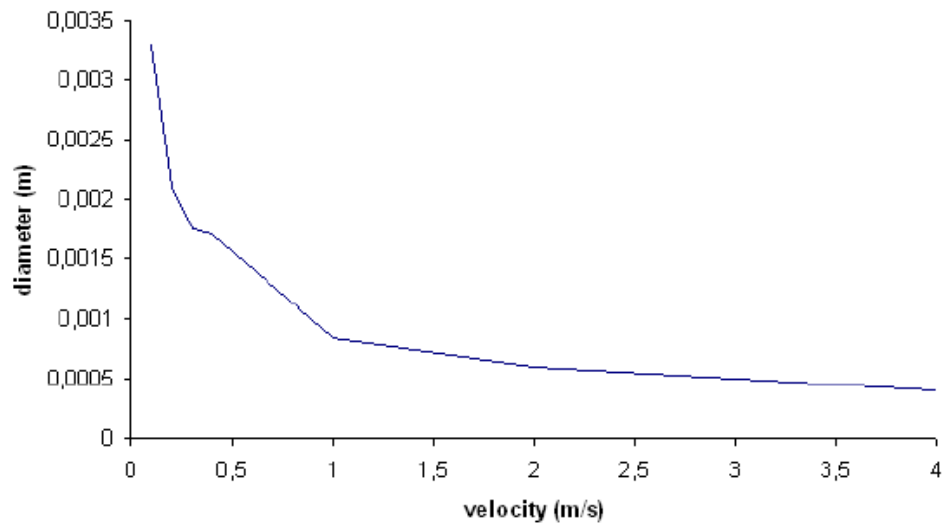


**Figure 2.10** Spatially averaged hydrate particle diameter as a function of mean velocity. (Fatnes, 2010)

## **CHAPTER 3**

### **METHODOLOGY**

This project is broken down into a few phases which need various methods to be carried out. Firstly, identification of problem and objective of project was carried out. Following that, phase 1 of the project was commenced which is project background study. It is then proceeded with research phase where ample studies and literature review was done. The project would then be continued with modeling stage. Multiphase model would be developed and analyzed using related software. The methodology involved for all project phases is explained at the few methodology breaks down below:

#### **3.1 Research Methodology**

At the beginning of the project, project background study was made by researches on related books, journals, research papers, internet articles and etc. Ample studies were done to understand the characteristics and behaviors of multiphase flow, narrowing down to the single phase and multiphase flow in pipes. At the same time, researches were done on hydrates composition, nature, characteristics, and condition of formation. The impacts of hydrates formation on the multiphase flow in pipes and the oil / gas transportation and production process were looked into, too.

After background study, project problem and objective identification, the project is go on with literature reviews on research papers previously done by researchers all over the world, earliest from the 1980's to the 2010's. The focus of the literature reviews includes effect of factors such as flow velocity, presence of inhibitor, and pressure variation on hydrates formation in pipes, relationship of heat transfer and hydrate formation or dissociation, boundary conditions and factors contributing to

hydrate formation, and numerical study on flow characteristics of Gas-Hydrate slurry two phase stratified flow. However, the literature reviews are not limited to the few focuses stated above as it changes and would be widen as the project goes on. Literature review would be constantly carried out throughout the project as an information gathering or data validation process.

## 3.2 Modeling Methodology

### 3.2.1 Geometry Setup

In the third phase of the project, modeling of the multiphase flow would begin. A 90 degree bend pipe of 45.2 mm diameter was modeled using ANSYS Designmodeler. The length of the horizontal pipe section was 450 mm and the vertical pipe section is 200 mm. The radius of the bend is 105 mm. The geometry used in the study is shown in Figure 3.1. Fluid will flow from the upper end of the vertical pipe through the bend and flow out through the horizontal pipe.

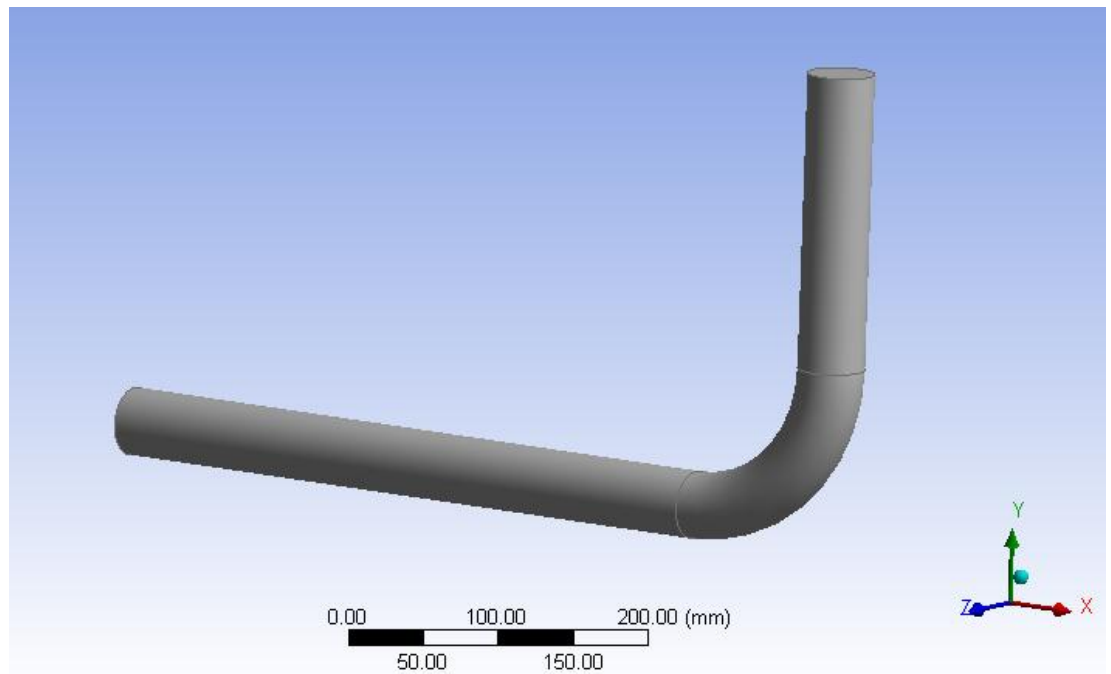


**Figure 3.1** The three-dimensional CAD-model used in the study.



### 3.2.2 Mesh Generation

Meshing is an important process in simulation because meshing allows the fluid flow to be analyzed better. With meshing, the flow domains would be split into smaller subdomains. The discretized governing equations are then solved inside each of the subdomains. Element-based finite volume method would be used via ANSYS CFX to mesh the pipe geometry into 15705 nodes and 70361 elements at an element size of 0.0044m with five inflated layers near the wall. However, the mesh dependency needs to be refined to obtain the most accurate result.

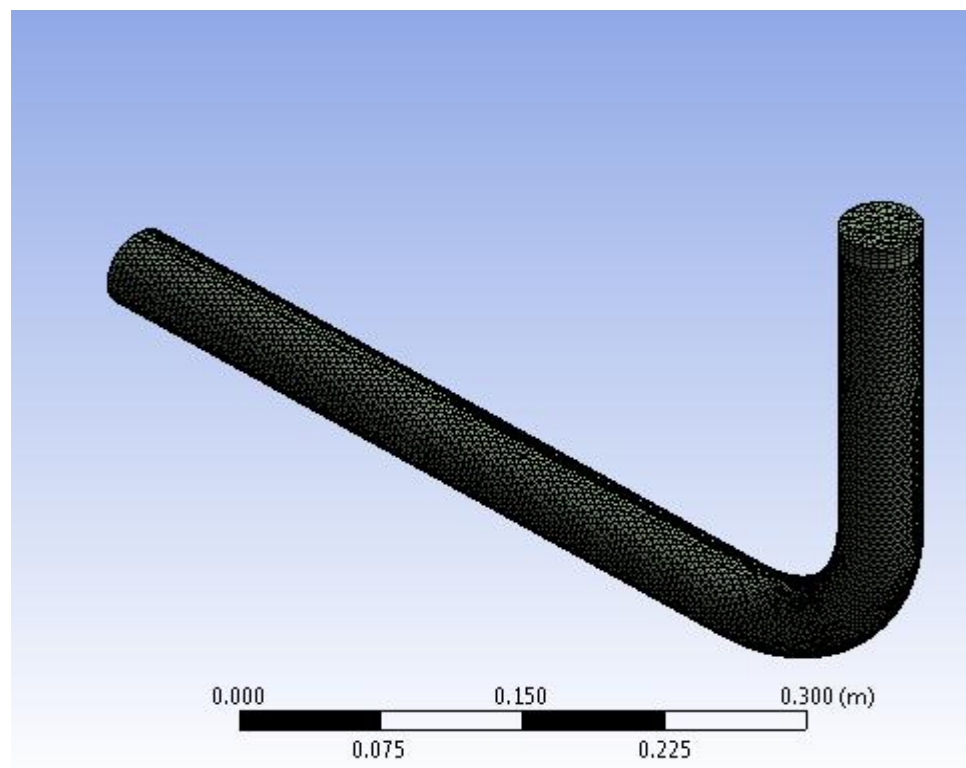


*Figure 3.2 Grid generation on the surface of the pipe.*

### 3.2.3 Fluid Setup

The model created is a two-fluid model created by defining the fluid properties. For the study, water was modeled as the continuous phase with a density of  $1000\text{kg/m}^3$ , molar mass of  $18.02\text{ g/mole}$  and viscosity of  $0.001\text{ Pa S}$ . The second fluid, Freon R11 hydrates were modeled as dispersed solid phase with a

density of 1140kg/m<sup>3</sup>, molar mass of 137.7g/mole, and viscosity 0.00321 Pa S. However, these properties of the Freon R11 Hydrates will be modified as the study reaches the stage of parametric analysis.

### 3.2.4 Multiphase Model

In this study, the multiphase flow in the pipe model is being modeled using the Eulerian-Eulerian two-fluid model. In other words, the multiphase flow is treated as turbulent and isothermal. The multiphase model is set to be inhomogeneous where each fluid has its own properties. For example, the two phases may have different velocity field, turbulence field and temperature fields. The fluids in an inhomogeneous model interact through interphase transfer terms.

Interfacial transfer of momentum, heat and mass depend on the contact area between the two phases involved in the model. This is measured by the interfacial area per unit volume, or the interfacial area density,  $A_{xy}$ , between the continuous phase and dispersed phase, named phase  $\chi$  and phase  $y$  accordingly. A particle model is used to model the interphase transfer between the continuous phase and the dispersed phase of hydrates. The surface area per unit volume is done based on the assumption that phase  $y$  is made up of spherical particles. From the particle model, the interfacial area density,  $A_{xy}$  is expressed as below:

$$A_{xy} = \frac{6\phi_y}{d_y} \quad (3.1)$$

Where,  $\phi_y$  is the volume fraction of the dispersed phase;  $d_y$  is the means diameter of the hydrates particles/dispersed particle.

Non-dimensional interphase transfer coefficients can be correlated in terms of the particle Reynolds number and the fluid Prandtl number [10].

$$Re_{xy} = \frac{\rho_x |U_y - U_x| d_y}{\mu_x} \quad (3.2)$$

$$Pr_{xy} = \frac{u_x c_{p,x}}{\lambda_x} \quad (3.3)$$

### 3.2.5 Boundary Conditions

Different boundary conditions were set at different location on the fluid model. At the pipe inlet, the velocities and the volume fractions for the continuous phase and dispersed phase were set. On the other hand, the pressure, which is the atmospheric pressure, at the outlet was specified. For the pipe wall, a no-slip wall condition was specified for the two phases.

### 3.2.6 Turbulence Model

A turbulence model is used to predict the effects of turbulence by simplifying the solution of the governing equations of turbulence. It is also defined as a computational procedure to ‘close’ the systems’ mean flow equations <sup>[4]</sup>.

In turbulence modeling of the continuous phase, the  $k$ - $\varepsilon$  model was used. A standard  $k$ - $\varepsilon$  model is a semi-empirical model which is based on model transport equations for the turbulent kinetic energy,  $k$  and the dissipation rate,  $\varepsilon$  <sup>[10]</sup>. It was assumed that the flow is fully turbulent and the effect of molecular viscosity is negligible.

On the other hand, a dispersed phase zero equation model was used for the dispersed solid phase in the study. The model relates the dispersed phase kinematic eddy viscosity,  $\nu_{td}$ , to the continuous phase kinematic eddy viscosity,  $\nu_{tc}$ , using a turbulent Prandtl number,  $\sigma$ . The relationship is shown in the expressions below:

$$\nu_{td} = \frac{\nu_{tc}}{\sigma} \quad (3.4)$$

### 3.2.7 Particle Model

The Particle Model is also known as the Solid Pressure Force Model where the forces due to solid collisions are considered by having additional solids pressure and solids stress terms into the solid phase momentum equations based on either the Gidaspow model or by specifying the elasticity modulus directly. In this work, the approach used to illustrate particle-particle interactions is through Gidaspow solid pressure model.

The radial distribution function,  $g_0$  which measures the probability of interparticle contact is given by Gidaspow model as below:

$$g_0(\phi_s) = 0.6 \left( 1 - \left( \frac{\phi_s}{\phi_{sm}} \right)^{-1} \right) \quad (3.5)$$

where  $\phi_{sm}$  is the volume fraction of the settled bed of solids,  $\phi_s$  is the volume fraction of the solid phase. The function in Equation 3.5 above becomes infinite when the in situ solids volume fraction approaches  $\phi_{sm}$ . The forces from solid collisions are considered by introducing additional solid pressure and solids stress terms into the solid phase momentum equation based on the Gidaspow model.

The equation below defines the coalitional solid stress tensor in the solid phase momentum equation.

$$\tau_{sij} = -P_s \delta_{ij} + \mu_s \left( \frac{\partial U_i}{\partial x_j} + \frac{\partial U_j}{\partial x_i} - \frac{2}{3} \frac{\partial U_k}{\partial x_k} \delta_{ij} \right) + \mathcal{E}_s \frac{\partial U_k}{\partial x_k} \delta_{ij} \quad (3.6)$$

where  $P_s$  is the solid pressure,  $\mu_s$  is the solids shear viscosity and  $\mathcal{E}_s$  is the solids bulk viscosity. The setting of the particle model is made at the Fluid Specific Model tab in ANSYS CFX.

### 3.3 Multivariate Regression Analysis

Regression analysis is a statistical process for estimating the relationships among variables. It is used for modeling and analyzing several variables, when the focus is on the relationship between a dependent variable and one or more independent variables. Besides, it helps on the understanding of how the typical value of the dependent variable changes when any one of the independent variables is varied, while the other independent variables are held fixed.

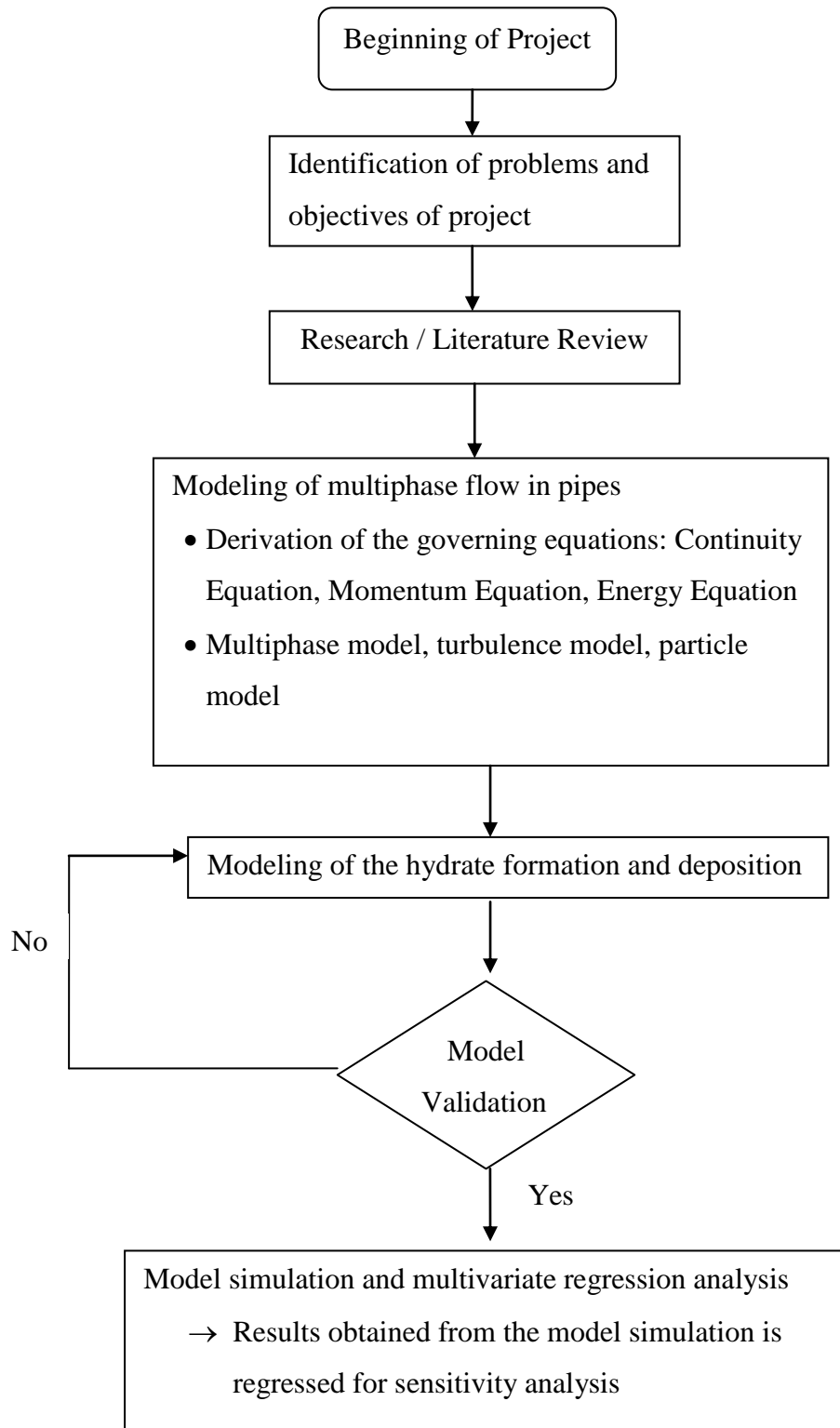
With the aid of Microsoft Excel solvers, an experimental design is developed using a second order regression method. The relationship between hydrates thickness formed and various factors would be analyzed through the regression to identify the most significant factors contributing to hydrate formation. Tornado diagram would be used

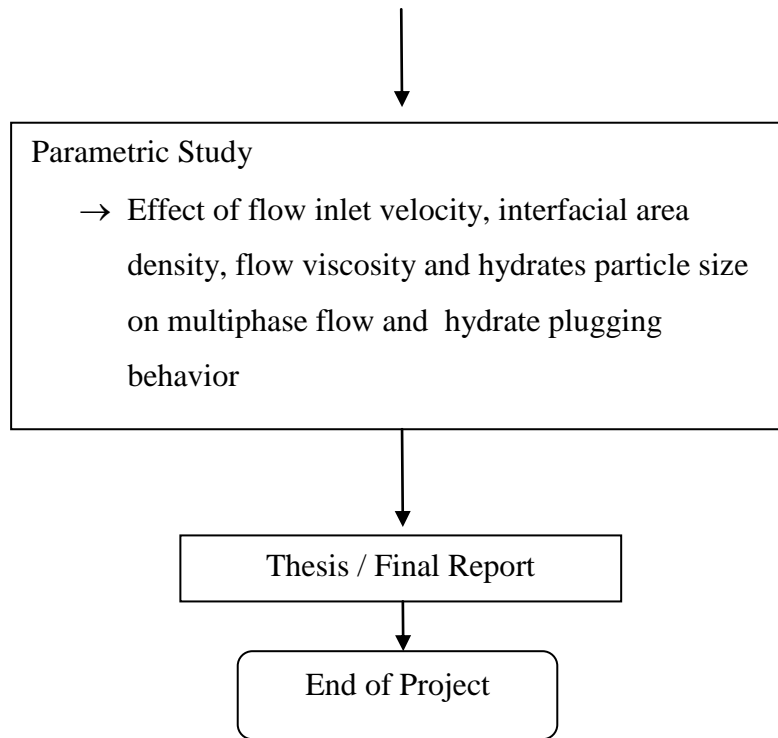
to illustrate the sensitivity of hydrate formation object to the factors within the scope of the study. Apart from this, bar chart would be plotted to show the significance of the various factors on hydrates formation.

### **3.3 Parametric Analysis**

Using the multiphase model developed, parametric analysis would be conducted by simulating the model in ANSYS CFX via various setting of the inlet mean flow velocity, hydrates viscosity, interfacial are desnity and hydrates particle size. With the aid of ANSYS CFX Solver and CFX-Post, the effect of inlet flow velocity and hydrates particles diameter on hydrates formation and plugging behavior in pipeline would be investigated. Graphs and various contours would be plotted using results extracted from ANSYS CFX and would further be interpreted as in results and discussion section.

### 3.4 Project Flow Chart





### 3.5 Gantt Chart

PROJECT ACTIVITIES	SEMESTER 1														SEMESTER 2														
	1	2	3	4	5	6	7	8	9	10	11	12	13	14	15	16	17	18	19	20	21	22	23	24	25	26	27	28	
Project Topic Selection	█	█																											
Identification of Problems and Objectives of Project			█																										
Background Study				█	█	█																							
Literature Review				█	█	█	█	█	█	█	█	█	█	█	█	█	█	█	█	█	█	█	█	█					
Modeling of Multiphase Flow in Pipe										█	█	█	█																
Modeling of hydrate formation and deposition											█	█	█	█	█	█													
Validation on Models											█	█	█	█	█	█													
Model Simulation and Multivariate Regression															█	█	█	█	█	█									
Parametric Analysis																					█	█	█	█	█	█			
Final Report																											█	█	█

Note:  Key Milestones



## **CHAPTER 4**

### **RESULTS AND DISCUSSIONS**

In this chapter, the results from the simulation of the hydrate formation in multiphase flow in a 90 degree elbow pipe using ANSYS CFX are presented. The results that will be presented below include the model validation results by comparing the results obtained with experimental study from Balakin *et al.* (2010) and research study by Eirik Daniel Fatnes (2010). After the model being validated, the study proceeds to regression analysis and lastly the parametric study. All results obtained would be discussed further.

The simulation done is on a two phase flow with water as the continuous phase and the Freon R11 Hydrates as the dispersed solid phase in an isothermal environment at 2 °C which is the temperature favorable for hydrates to form. The regression analysis shows the significance and sensitivity of various factors affecting hydrate formation in the multiphase flow pipe. Parametric study would investigate the effect of interfacial area density, particle size of the hydrates particles, flow inlet velocity and the flow viscosity on the hydrate formation. The results obtained from simulation are extracted and plotted in graphs to illustrate the effect of the various factors on hydrates formation more clearly.

#### **4.1 Model Validation Results and Discussion**

Using ANSYS CFX, a model of multiphase flow in pipe which consists of water as the continuous fluid and Freon R11 hydrates as the dispersed solid was built. To make sure that the model is valid for further parametric studies, validation was done

on the model based on an experimental study from Balakin *et al.* (2010) [21] and research study by Eirik Daniel Fatnes (2010) [10].

Particle deposition is the natural attachment of particles to surfaces, mainly due to gravitational force acting on it. In oil and gas industries, hydrates particle deposition in pipelines would increase the pressure drop of the flow, leading to plugging of the pipeline as the hydrates particles gradually aggregate.

Mean Velocity (m/s)	Hydrate Particle Size (m)
0.1	0.0033
0.2	0.0020
0.3	0.0018
0.4	0.0017

**Table 4.1** Sets of input data used in ANSYS CFX simulation of hydrate formation and deposition.

In the simulation conducted which aims to model the hydrate formation and deposition in the pipe studied, different inlet mean velocities of the flow were used as the inlet boundary conditions, following with the respective hydrate particle mean diameter for the dispersed phase. The input data are summarized in the Table 4.1 above.

Summarizing the results obtained from study by Eirik Daniel Fatnes (2010) and experimental work by Balakin *et al.* (2010), a graph of hydrate precipitates thickness against mean flow velocity is plotted as shown in Figure 4.9. The hydrate precipitates thickness from the ANSYS CFX simulation in this study is extracted and plotted on the graph.

Comparing the results produced by Eirik Daniel Fatnes (2010) and experimental work by Balakin *et al.* with the current results, it is observed that in all three set of results obtained the hydrates precipitation or the hydrate volume fraction near the wall decreases as the mean flow velocity increases from 0.1 m/s to 0.4 m/s.

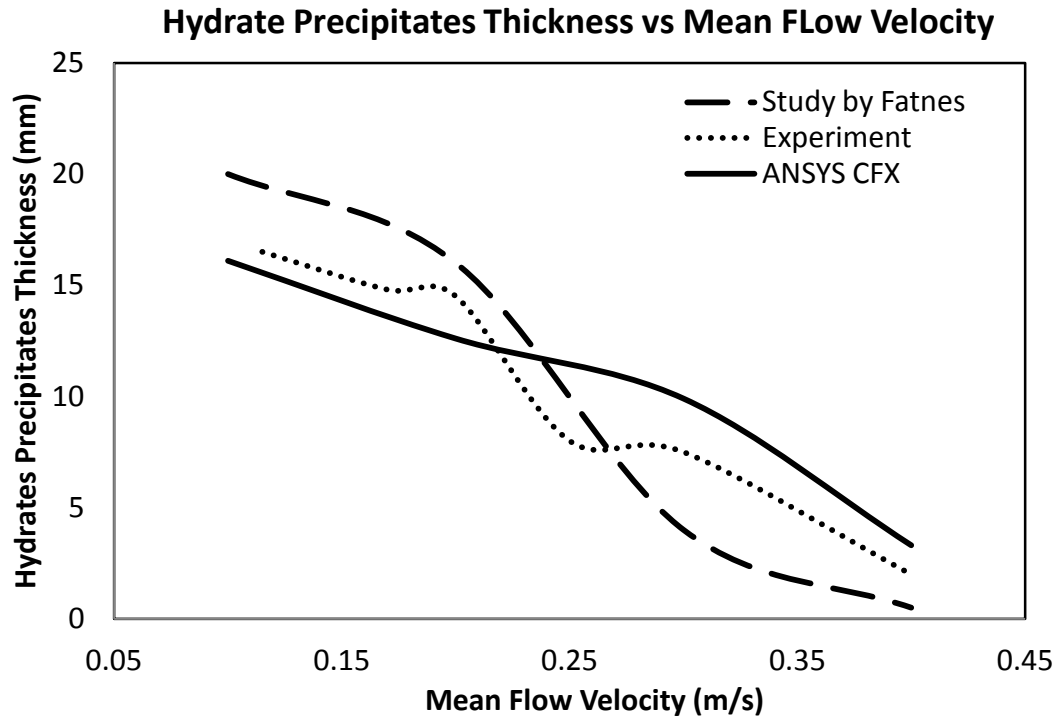


**Figure 4.1** Graph of hydrate precipitates/bed thickness against mean flow velocity. Comparison of ANSYS CFX, experimental data and study by Fatnes.

On the whole, the results from ANSYS CFX simulation is in good agreement with the experimental work of Balakin *et al.* over the whole velocity range. The slight differences in the results between ANSYS CFX and the experiment are mainly due to several reasons. Firstly, the mesh generation and discretization in the CFX simulation could never be the same as the set up in real experiment. In this study, the model only includes geometry of an elbow pipe which is a part of the experimental loop whereas in the experiment, the fluid flows through a series of bends and equipments such as pumps and valves.

## 4.2 Regression Analysis

There are a large number of parameters involved in this study as hydrates formation is a complicated mechanism which behavior is rarely recognized or reported. Moreover, in oil and gas industries from drilling process to production in plant, the fluid flow is made up of vast mixture of various gasses, liquid, and solid particles flow, making the control over hydrates formation even more complicated due to the large amount of possible factors. Thus, an experimental design was developed using a second order regressed method.

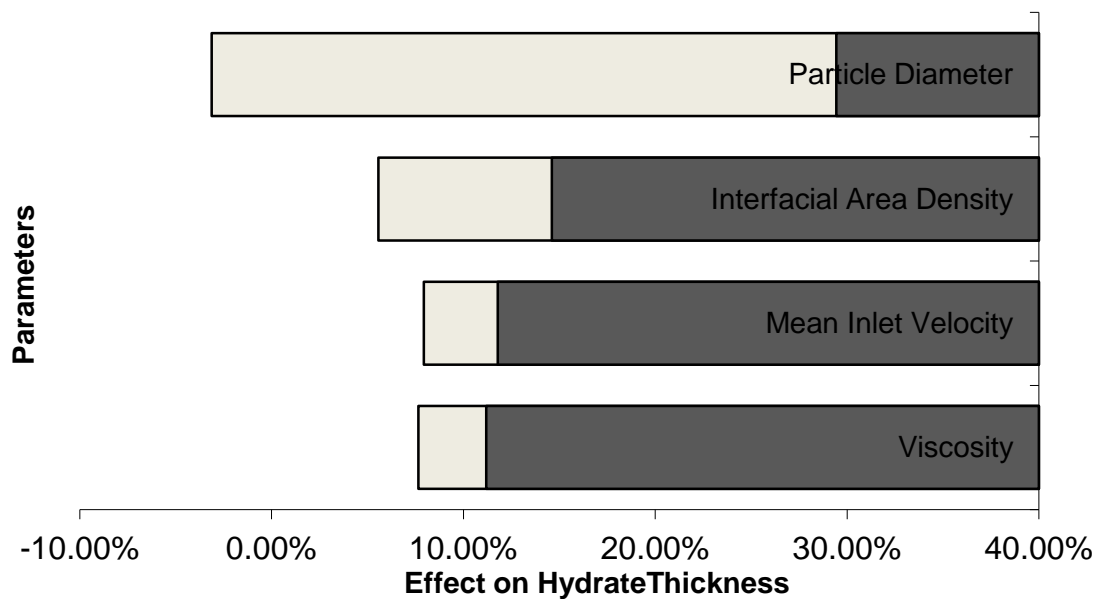


*Figure 4.2 Sensitivity of different parameters to hydrate thickness formed in multiphase flow pipe. Results obtained from experimental design and second order regression.*

A tornado chart is constructed as shown in Figure 4.2 for sensitivity analysis. From the tornado chart, the longer the bar the greater the sensitivity of hydrate formation object to the factor and vice versa. Starting from the top, particle size of the flow has the greatest impact following by interfacial area density, mean inlet velocity, and flow viscosity. Both ends of the bars indicate the minimum and maximum effect of the factors. For instance, the size of the particles in the flow have an impact of up to

3000% maximum increase on the hydrates thickness while a proper control on the particles' diameter can prevent the hydrates formation which is shown on the minimum end of the bar.

From the sensitivity analysis, it is noted that a careful control over particle size of the hydrates particles and interfacial area density is crucial to reduce or prevent hydrate formation. On the other hand, the other two factors which are the flow inlet velocity and flow viscosity are less significant thus less emphasize on the two factors is acceptable in cases of insufficient time or budget on hydrates mitigation and remediation planning.

Using the multiphase flow model built in ANSYS CFX, a total of four factors are predicted to be affecting hydrate formation in multiphase flow pipe. With the aid of second order regressed method, the graphs in Figure 4.3 are plotted. Those variables are flow viscosity, particle size, inlet velocity of the flow, and interfacial area density. These variables are regressed to a second order to investigate the stability and significance of each factor on hydrate formation. In Figure 4.3, it shows the influence percentage for each variable upon the hydrate thickness formed in the pipe. Out of all factors, particle size of the solid dispersed phase in the flow significantly influences the hydrates thickness formed up to 2500%. It is then followed by influence from the flow inlet velocity and interfacial area density, both with an influence percentage upon hydrates thickness of around 800%. Influence from flow inlet velocity is slightly higher than that of interfacial area density. Flow viscosity has the least influence on the hydrate thickness formed among all the factors. The effect of the factors on hydrate formation would be further discussed in the following section.

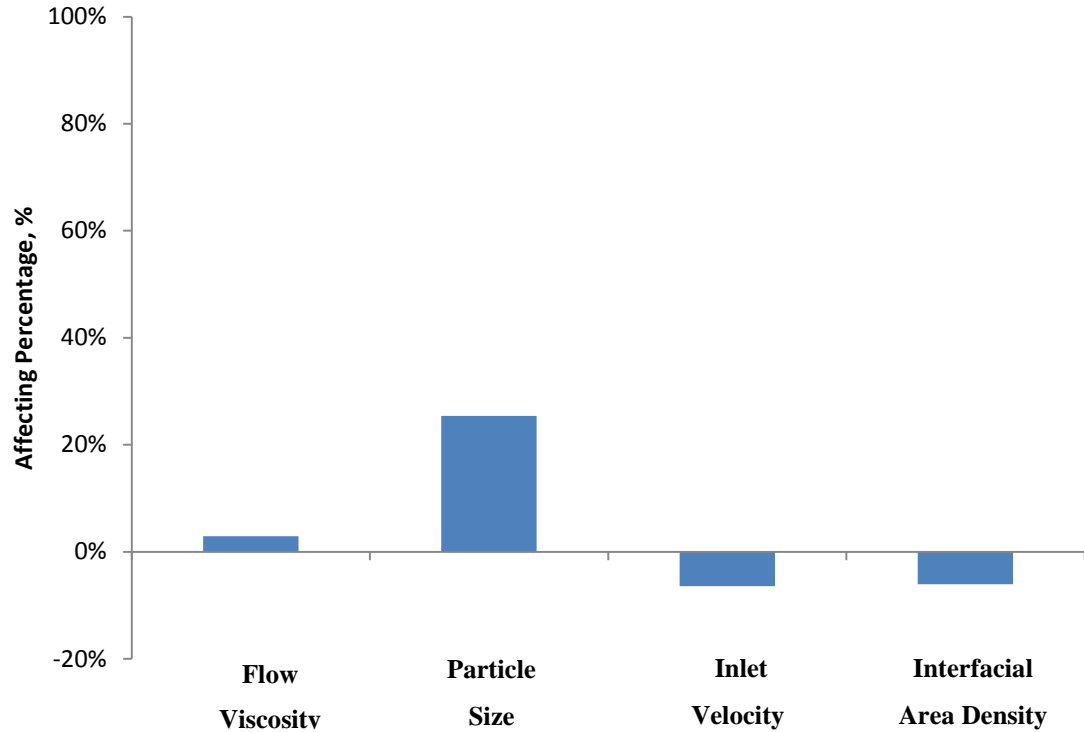


*Figure 4.3 Significance of factors on hydrates thickness formed in the pipe.*

### **4.3 Hydrate Formation and Deposition Simulation**

In the current study, the geometry model used in the simulation is a 90 degree bend pipe to model the multiphase flow and hydrate formation in the pipe. This section would discuss the hydrate formation and deposition process in different sections of the pipe.

The bend and obstructions in a 90 degree bend pipe cast impacts on the hydrate formation and deposition process. In the simulation done, the velocity of the continuous phase is being investigated, too apart from the hydrate formed in the pipe. Figure 4.4 shows the contour of hydrates volume fraction at midline cross-section of the pipe for one of the simulation conducted whereas Figure 4.5 is the contour of the water speed at midline cross-section of the pipe.

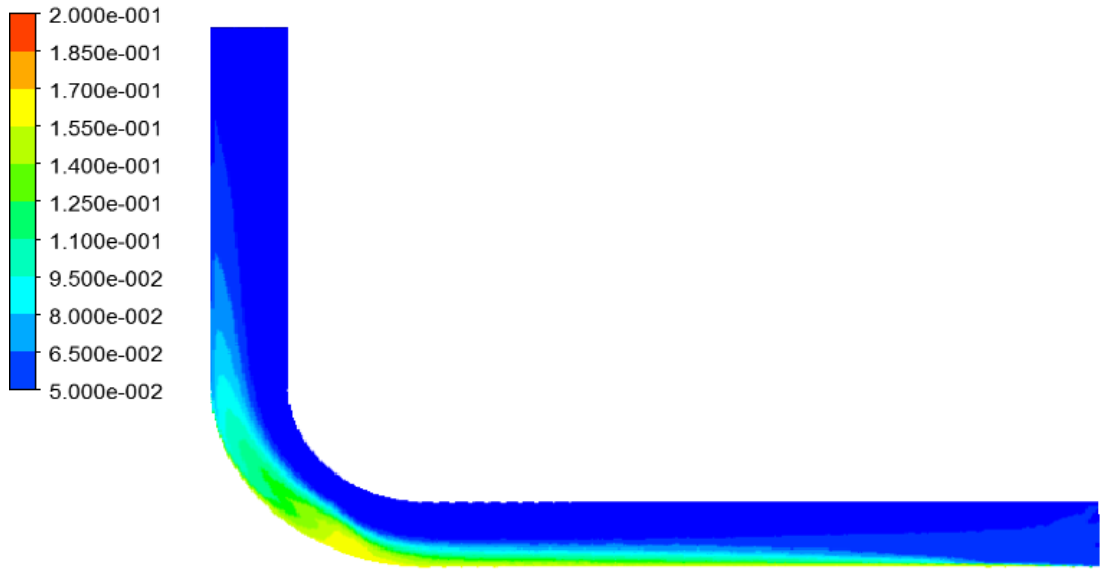


**Figure 4.4** Contour of the hydrate volume fraction at midline cross-section of the pipe. Mean inlet velocity of 0.1 m/s, particle size of 0.0033 m.

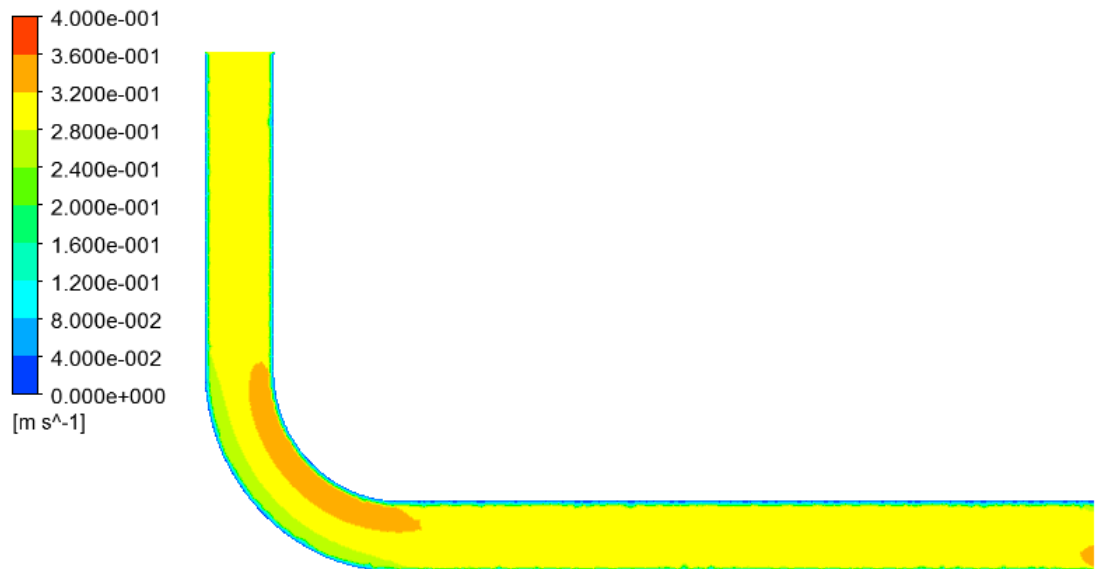


**Figure 4.5** Contour of the water (continuous phase) speed at midline cross-section of the pipe. Mean inlet velocity of 0.3 m/s, particle size of 0.0035 m, interfacial area density of 0.075 and viscosity of 0.0061.

From Figure 4.5, it can be observed that the highest speed of the continuous phase is at the inner part of the bend which is denoted by an orange color contour. The water speed is the lowest at the lower horizontal region. This observation is mainly due to the hydrates formed at the bottom of the inner pipe wall which causes obstruction to the flow. It is also noticed that the lowest speed denoted by the blue colour contour along the inner walls boundary. This could be explained by the no-slip boundary condition at the pipe wall where the water speed has zero velocity relative to the boundary.

On the other hand, from Figure 4.4, there is a higher volume fraction of hydrates at the bend than the horizontal section of the pipe. Apart from this, it is also observed that there is a higher hydrate volume fraction at the bend's outer section. This indicates that the particle concentration is at a maximum at the outer section bend of the pipe. When the fluid flows through the 90 degree bend section, there is a centripetal acceleration which acts radially inwards. Pressure near the outer wall of the bend would increase whereas the pressure near the inner wall of the bend would decrease. As the fluid flow through the pipe from the vertical end through the 90 degree bend to the horizontal end of the pipe, the flow experiences an adverse pressure gradient where the pressure increases in the direction of flow. Due to this, the hydrates particles in the flow are influenced by their close proximity to the wall. The hydrates particles would have low velocities and unable to overcome the adverse pressure gradient, causing a separation of flow from the boundary. Apart from this, as shown in Figure 4.5 the water speed is lower at the bend. A lower velocity then give rise to more hydrates precipitation at the pipe wall and eventually lead to hydrate plugging of the pipe.



#### 4.4 Effect of Hydrate Particle Size on Hydrates Formation

Particle size is the most influential factor in the current study based on the regression analysis. In order to investigate the effect of hydrate particle size on hydrates formation, simulations were done using Gidaspow solid pressure model at three different conditions: i) 0.00465 kg/ms viscosity, minimum interfacial area density of 0.063, 0.2m/s to 0.4m/s inlet velocity; ii) 0.00755 kg/ms viscosity, minimum interfacial area density of 0.088, 0.2m/s to 0.4m/s inlet velocity; iii) 0.00610 kg/ms viscosity, minimum interfacial area density of 0.075, 0.1m/s to 0.5m/s inlet velocity

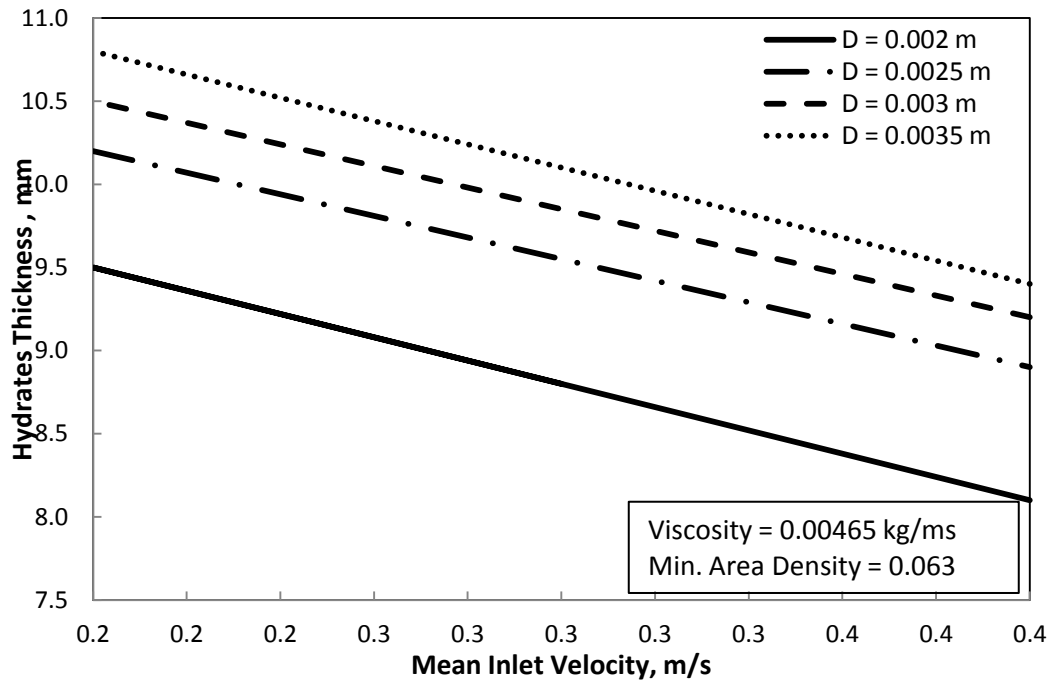


*Figure 4.6 Effect of hydrates particle size on hydrates thickness for condition i.)*

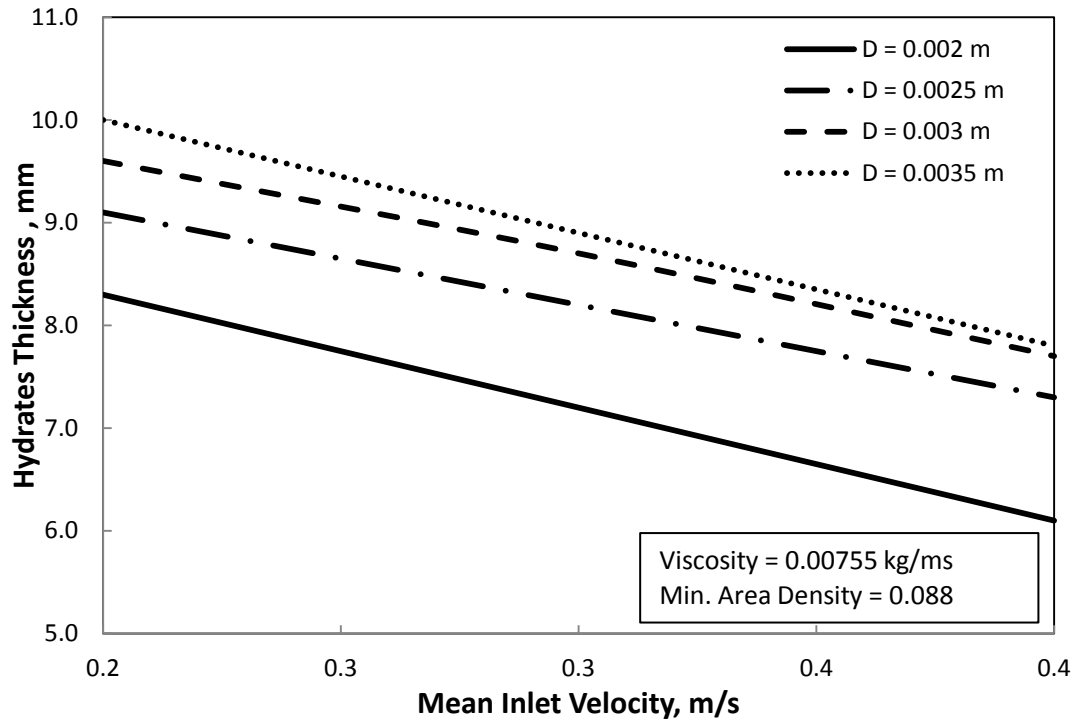


Figure 4.7 Effect of hydrates particle size on hydrates thickness for condition ii.)

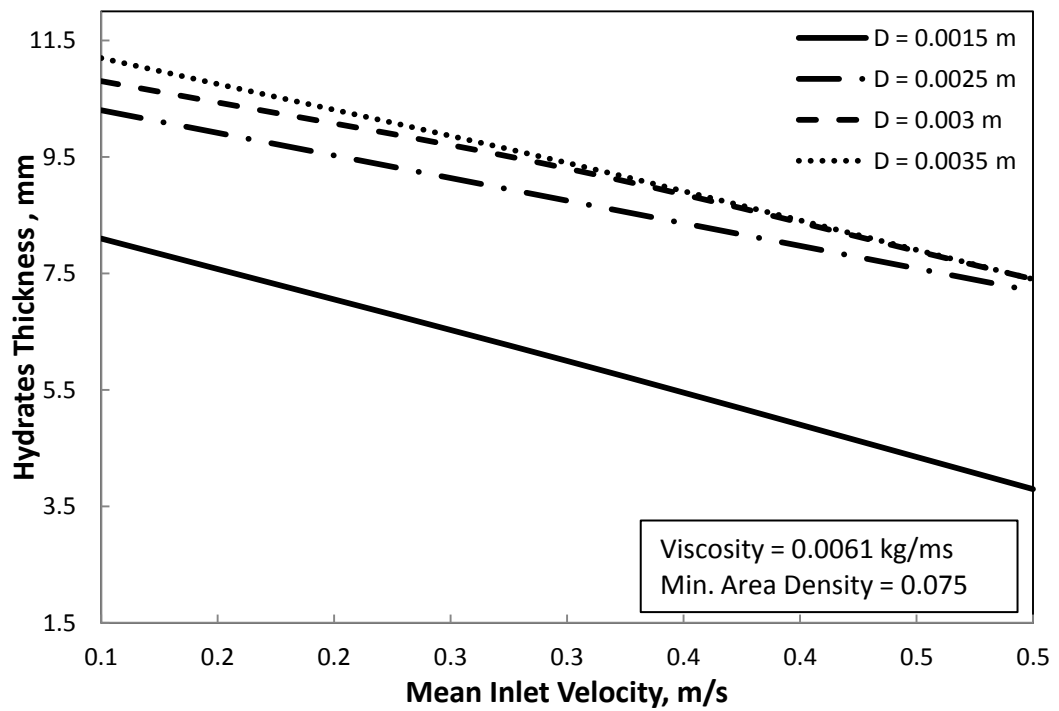


Figure 4.8 Effect of hydrates particle size on hydrates thickness for condition iii.)

Based on the graphs in Figure 4.6 to 4.8, it is shown that the hydrates thickness increases with increasing particle size. This could be explained by the terminal velocity given by the equation below:

$$U_t = \frac{1}{18} \frac{(\rho_s - \rho_l)}{\mu_l} d^2 g (1 - \phi_s)^5 \quad (4.1)$$

Where,  $\rho_s$  is the density of hydrates particle,  $\rho_l$  is the density of the water,  $\mu_l$  is the water viscosity,  $d$  is the hydrate particle diameter,  $\phi_s$  is the hydrates volume fraction, and  $g$  is the gravitational acceleration (Fatnes E. D., 2010). Terminal velocity is the speed in which a particle subsides and deposited. As shown in Equation 4.1, terminal velocity is directly proportional to particle size, causing the hydrates thickness to increase with increasing particle size. In other words, the rate of hydrates deposition increases with the increasing particle size.

#### **4.5 Effect of Interfacial Area Density on Hydrates Formation**

Interfacial area density,  $A$  is also characterized as interfacial area per unit volume between two phases in a flow which indicates the transfer of momentum, heat and mass between the phases. In the model simulation of the current study, control over the interfacial transfer is done by settings on minimum volume fraction for area density in a Particle Model. The Particle Model provides the algebraic prescriptions for the interfacial area density. Assumption made in Particle Model is one of the phases is continuous, which is water phase for this study, and the other phase is dispersed, which is the Freon R11 Hydrate phase.

The graphs in Figure 4.9 to Figure 4.11 were plotted by using the results extracted from ANSYS CFX. Based on all three graphs, it is observed that a higher interfacial area density of the fluid gives a lower hydrate thickness. From the negative gradient on the plot on Figure 4.9 and 4.10, it can be seen that the higher interfacial area density decreases the rate of hydrate formation. A similar fluid viscosity but a lower particle diameter causes the hydrate thickness to decrease 1mm which is quite drastic.

On the other hand, in Figure 4.10 and Figure 4.11, a different viscosity but similar particle diameter of 0.002m only reduces 0.25mm of the hydrates thickness. This observation is a proof on the finding in section 4.2 where particle diameter has the most significant impact on hydrate formation. As a conclusion for this section, increase in interfacial area density between two phases will decrease the rate of hydrate formation. The effect from viscosity on hydrate formation would be discussed in following section 4.7.

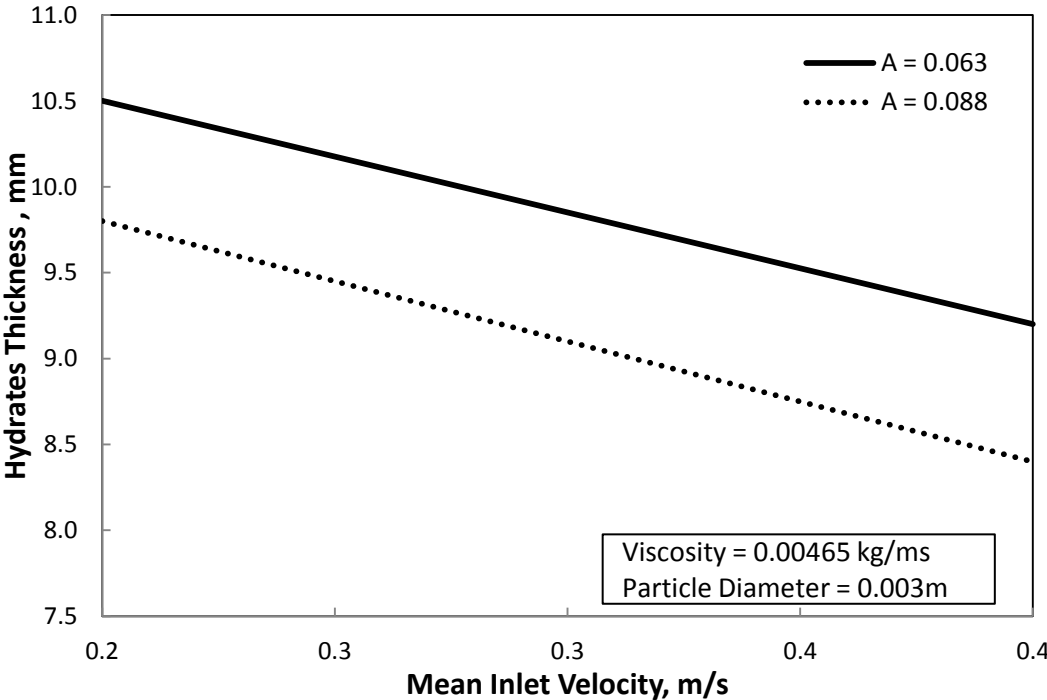


**Figure 4.9** Effect of interfacial area density on hydrates thickness for 0.00465 kg/ms viscosity, 0.003m particle diameter, 0.2m/s to 0.4m/s inlet velocity

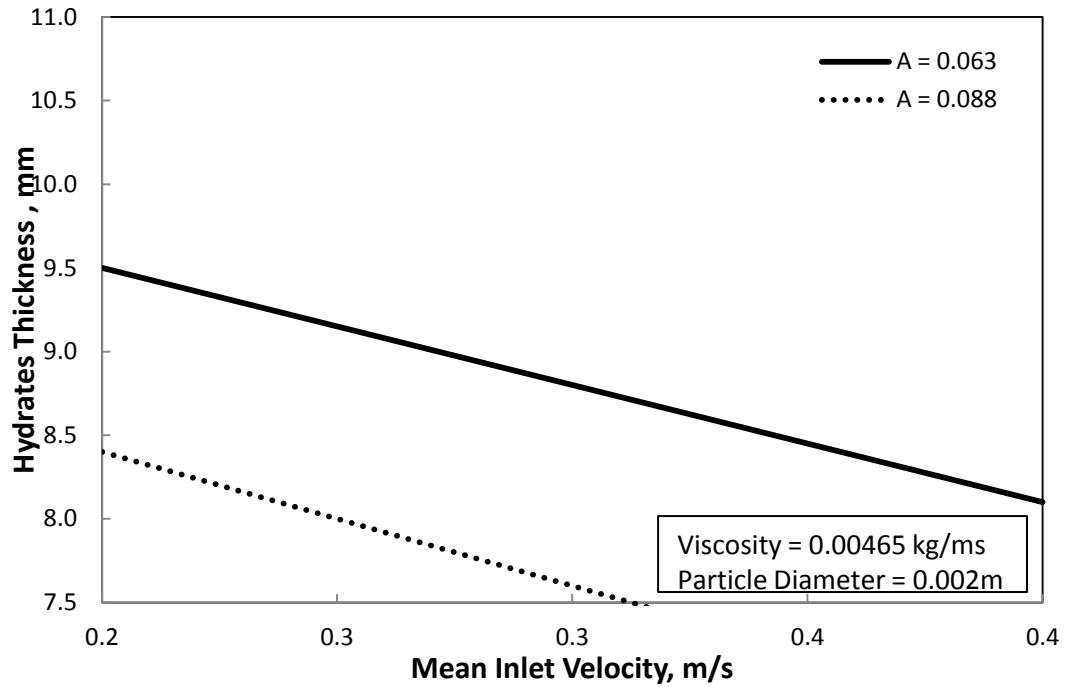


**Figure 4.10** Effect of interfacial area density on hydrates thickness for 0.00465 kg/ms viscosity, 0.002m particle diameter, 0.2m/s to 0.4m/s inlet velocity

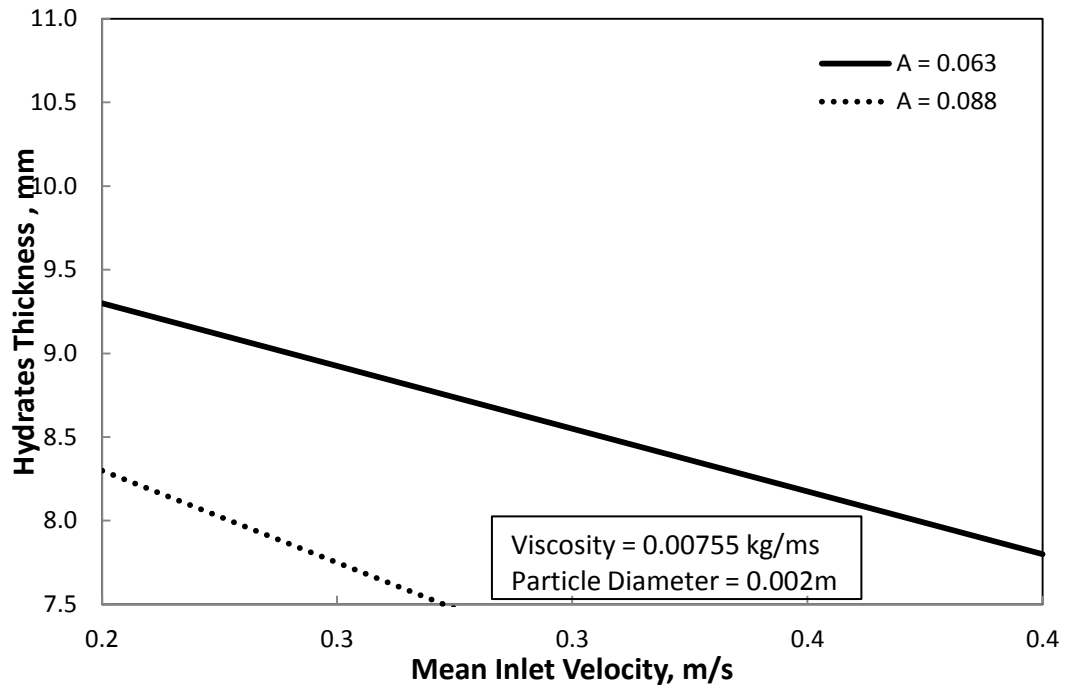


**Figure 4.11** Effect of interfacial area density on hydrates thickness for 0.00755 kg/ms viscosity, 0.002m particle diameter, 0.2m/s to 0.4m/s inlet velocity

#### **4.6 Effect of Inlet Velocity on Hydrates Formation**

Flow inlet velocity is a crucial factor in oil and gas industries as it could be monitored easily with the aid of pumps and compressors. Moreover, inlet velocity of a flow affects the efficiency and productivity of the industries as a proper control over the flow velocity would save plenty of time. Therefore, it is necessary for us to look into the impact of inlet velocity on hydrates formation in order to prevent hydrates plugging that would lower the industries' productivity.

In the current study, simulations are done in the range of inlet velocity of 0.1 m/s to 0.5 m/s. At the end of simulations, the results are extracted and plotted into graphs in Figure 4.12 to Figure 4.14. A trend of higher inlet velocity gives a lower hydrate thickness is observed from all three graphs. Such phenomenon is due to the flow patterns in solid-liquid flow in the current study. At a lower inlet velocity, the solid-liquid flow is becoming a flow with stationary hydrates bed. This is because a lower inlet velocity has a lower ability to enable motion of the immersed hydrates particles formed in the pipe. Thus, the hydrates particles deposits and increases the hydrates thickness. In contrast, a higher inlet velocity enables the solid-liquid to flow with a moving hydrates bed. Despite of the aggregation of the hydrates particles over time, the hydrates particles which accumulate at the bottom of pipe would form a packed bed layer and is able to move along the pipe bottom with the aid of a higher flow rate of water phase (continuous phase). Due to this, a higher inlet velocity would give a lower hydrate thickness formed in the pipe.

Besides that, as the particle diameter increases to 0.003m, the effect from flow inlet velocity on the hydrates thickness decreases. This is portrayed by the gradually flatten lines on the graph which indicates that the gradient is zero or in other words, the rate of change of hydrates thickness over change in particle diameter is zero.

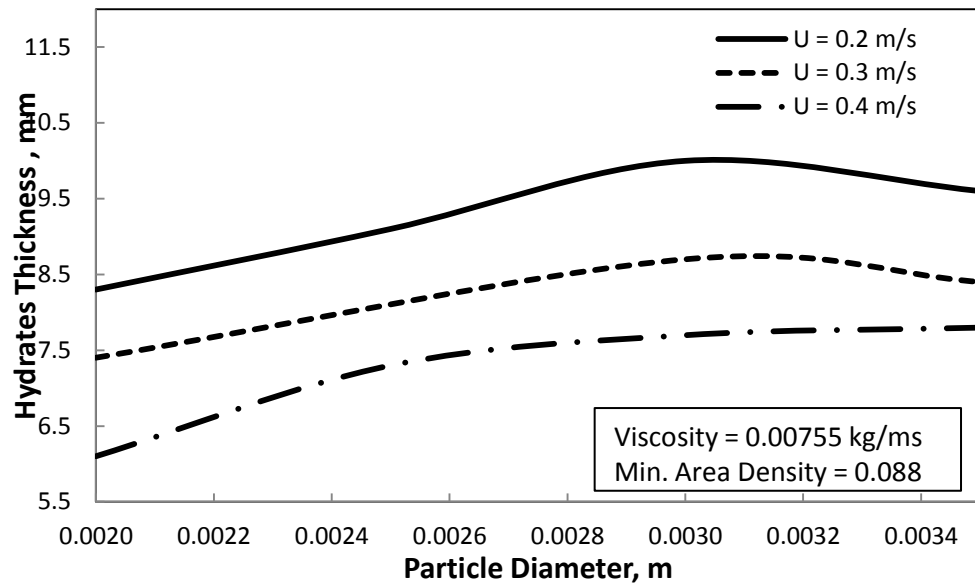


**Figure 4.12** Effect of inlet velocity on hydrates thickness for 0.00755 kg/ms viscosity, 0.002m to 0.0035m particle diameter, 0.088 min. area density

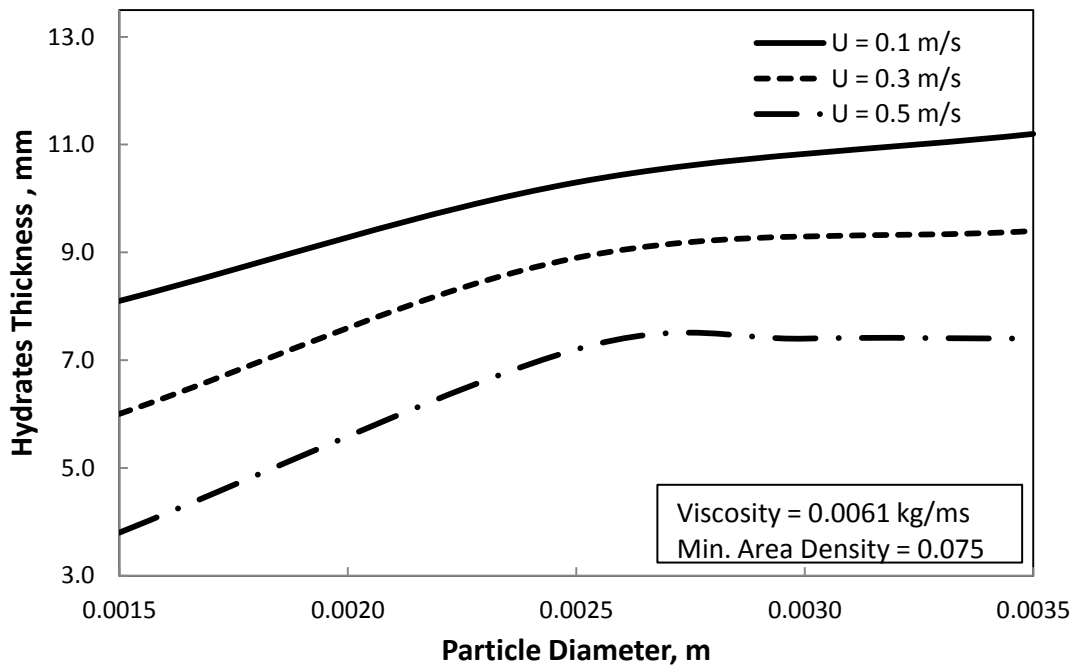


**Figure 4.13** Effect of inlet velocity on hydrates thickness for 0.00610 kg/ms viscosity, 0.0015m to 0.0035m particle diameter, 0.075 min. area density

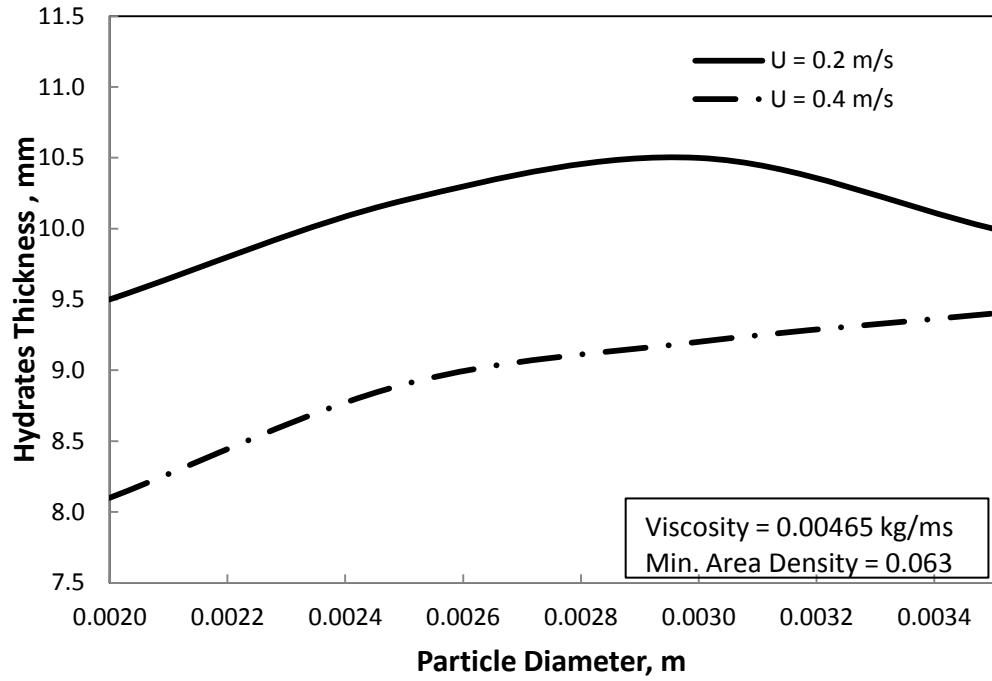


**Figure 4.14** Effect of inlet velocity on hydrates thickness for 0.00465 kg/ms viscosity, 0.002m to 0.0035m particle diameter, 0.063 min. area density



## **CHAPTER 5**

### **CONCLUSION AND RECOMMENDATION**

In oil and gas industries, hydrates formation in multiphase flow pipelines leading to pipe plugging had been a serious issue. Moreover, hydrates formation is a complicated mechanism which behavior is rarely reported. Thus, it is important to study on hydrates formation in multiphase flow pipe and the factors affecting it. In the current study, the factors being studied are size of the particles in the flow, interfacial area density, inlet velocity and flow viscosity.

In a nutshell, hydrates plugging in pipelines are governed by hydrates particles size, interfacial area density, flow inlet velocity and flow viscosity, with an increasing order of its significance on hydrates formation around the pipe circumference. To prevent hydrates formation and plugging, the fluid flow should be maintained at a high inlet velocity with minimum particle size. The two objectives of the study had been achieved.

Mitigation steps and remediation of hydrates should be emphasized in oil and gas project planning in order to prevent hydrate plugging. As mentioned in the findings from the study, hydrate particle diameter has the most influence on hydrates formation. Hydrate plugging can be prevented by applying depressurization where a hydrate plug is depressurized simultaneously from both ends. Depressurization will cause the hydrates to dissociate and reduces the hydrate particles diameter until the solid hydrate phase is depleted. Other hydrate prevention method includes hydrate control through water removal by removing the host water molecules, hydrate control through thermodynamic inhibition chemicals, and injection of anti-

agglomerants. According to the findings in section 4.3, fluid flow through a pipe bend is more prone to hydrates formation and plugging due to the adverse pressure gradient occurs at the bend. Thus, in the process of designing and constructing oil and gas pipelines, pipe bend should be avoided whenever possible to lower the risk of hydrates plugging.

For future studies, more parameters such as pipe diameter and pipe orientation should be investigated. Optimization should be done using solver to predict the optimum condition for a multiphase flow in pipelines to avoid hydrates formation/plugging.

## REFERENCES

- [1]. Abay, H. K. (2011). *Kinetic of Gas Hydrate Nucleation and Growth*. Stavanger : University of Stavanger.
- [2]. Andersson, V. (1999). *Flow Properties of Natural Gas Hydrate Slurries- An Experiemental Study*. Norwegian University of Science and Technology, Petroleum Engineering and Applied Geophysics. Norway: Norwegian University of Science and Technology.
- [3]. Balakin, B. V. (2010). *Experimental and Theoretical Study of the Flow, Aggregation, and Deposition of Gas Hydrate Particles* . Bergen: University of Bergen .
- [4]. Barker, A. (2012, March 4). *Applied Computational Fluid Dynamics*. Retrieved April 9, 2013, from The Colourful Fluid Mixng Gallery : <http://www.bakker.org/dartmouth06/engs150/10-rans.pdf>
- [5]. Bratland, O. (2010). Hydrates . In O. Bratland, *Pipe Flow 2: Multi-phase Flow Assurance* (pp. 275 - 284).
- [6]. Cahill, J. (2011, January 25th). *Avoiding Hydrate Formation in Offshore Gas Wells*. Retrieved February 6th , 2013, from Emerson Process Experts : [http://www.emersonprocessxperts.com/2011/01/avoiding\\_hydrat/#.URIjjB1weR8](http://www.emersonprocessxperts.com/2011/01/avoiding_hydrat/#.URIjjB1weR8)
- [7]. Christiansen, H. E. (2012). *Rate of Hydrate Inhibitor at Long Subsea Pipelines*. Trondheim : Norwegian University of Science and Technology .
- [8]. Donohue, D. (2000). Effects of Hydrate Formation on Gas Composition: A physical chemistry and environmental science question.
- [9]. Dorstewiz, F., & Mewes, D. (1995). Hydrate Formation in Pipelines. *Fifth International Offshore and Polar Engineering Conference*, (pp. 244-249). Hague, Netherlands.
- [10]. Fatnes, E. D. (2010). *Numerical Simulations of the Flow and Plugging Behavior of Hydrate Particles*. University of Bergen, Physics and Technology . Bergen: University of Bergen.

- [11]. Gong, J., & Zhao, J.-K. (2008). Numerical Simulation of Gas-Hydrate Slurry Two Phase Flow. *6th International Conference on Gas Hydrates (ICGH 2008)*. Vancouver, Canada.
- [12]. Gong, J., Shi, B., & Zhao, J. (2010). Natural Gas Hydrate Shell Model in Gas-Slurry Pipeline Flow. *Journal of Natural Gas Chemistry* , 19 (3), 261-266.
- [13]. Gong, J., Shi, B., Wang, W., & Zhao, J. (2010). Numerical Study the Flow Characteristics of Gas-Hydrate Slurry Two Phase Stratified Flow. Beijing, Changping, China.
- [14]. Jassim, E., Abdi, M. A., & Muzychka, Y. (2010). A New Approach to Investigate Hydrate Deposition in Gas-Dominated Flowlines. *Journal of Natural Gas Science and Engineering 2 (2010)* , 163-177.
- [15]. Lee, J.-H., Baek, Y.-S., & Sung, W.-M. (2002, September 10). Effect of Flow Velocity and Inhibitor on Formation of Methane Hydrates in High Pressure Pipeline. Incheon 406-130, Korea.
- [16]. Lippmann, D., Kessel, D., & Rahimian, I. (1995). Gas Hydrate Nucleation and Growth Kinetics in Multiphase Transportation Systems. *Fifth (1995) International Offshore and Polar Engineering Conference. 1*, pp. 250-256. Hague: The International Society of Offshore and Polar Engineers.
- [17]. Liu, B., Pang, W., Peng, B., Sun, C., & Chen, G. (2011, September 15). Heat Transfer Related to Gas Hydrate Formation/Dissociation. Beijing 102249, China.
- [18]. PetroMin PIPELINER. (2011). *Flow Assurance - Special Focus on Hydrate Blockage*.
- [19]. Sloan Jr, E. D. (2000). Prevention by Design: How to Ensure that Hydrates Won't Form. (J. B. Bloys, Ed.) *Hydrate Engineering* , 10-12.
- [20]. Sloan Jr, E. D. (2000). Prevention by Design: How to Ensure that Hydrates Won't Form. (J. B. Bloys, Ed.) *Hydrate Engineering* , 4-6.
- [21]. Balakin, B., Pedersen, H., Kilinc, Z., Hoffmann, A., Kosinski, P., & Hoiland, S. (2010). Turbulent Flow of Freon R11 Hydrate Slurry . *Journal of Petroleum Science and Engineering 70* , 177-182 .
- [22]. K. Mühle, *Floc stability in laminar and turbulent flow: Coagulation and Flocculation: Theory and Application (B. Dobias, Ed.)*, *Surfactant Science Series*, vol. 47. Acad. Press., 1993.

- [23]. R. Durand, "Basic relationships of the transportation of solids in pipes: Experimental research," in *Proceedings of the 5th Congress, International Association of Hydraulic Research*, 1953.
- [24]. E. J. Wasp, T. C. Aude, J. P. Kenny, R. H. Seiter, and R. B. Jaques, "Deposition velocities, transition velocities and spatial distribution of solids in slurry pipelines," in *Proceedings of the 1st International Conference on the Hydraulic Transport of Solids in Pipes (Hydrotransport 1)* (U. BHRA Fluid Engineering: Cran\_eld, ed.), no. Paper H4, pp. 53-76, 1970.